



DARK ENERGY
SURVEY

Review of Photometric Redshifts and Application to the Dark Energy Survey

Huan Lin, Fermilab



Photometric Redshifts

DARK ENERGY
SURVEY

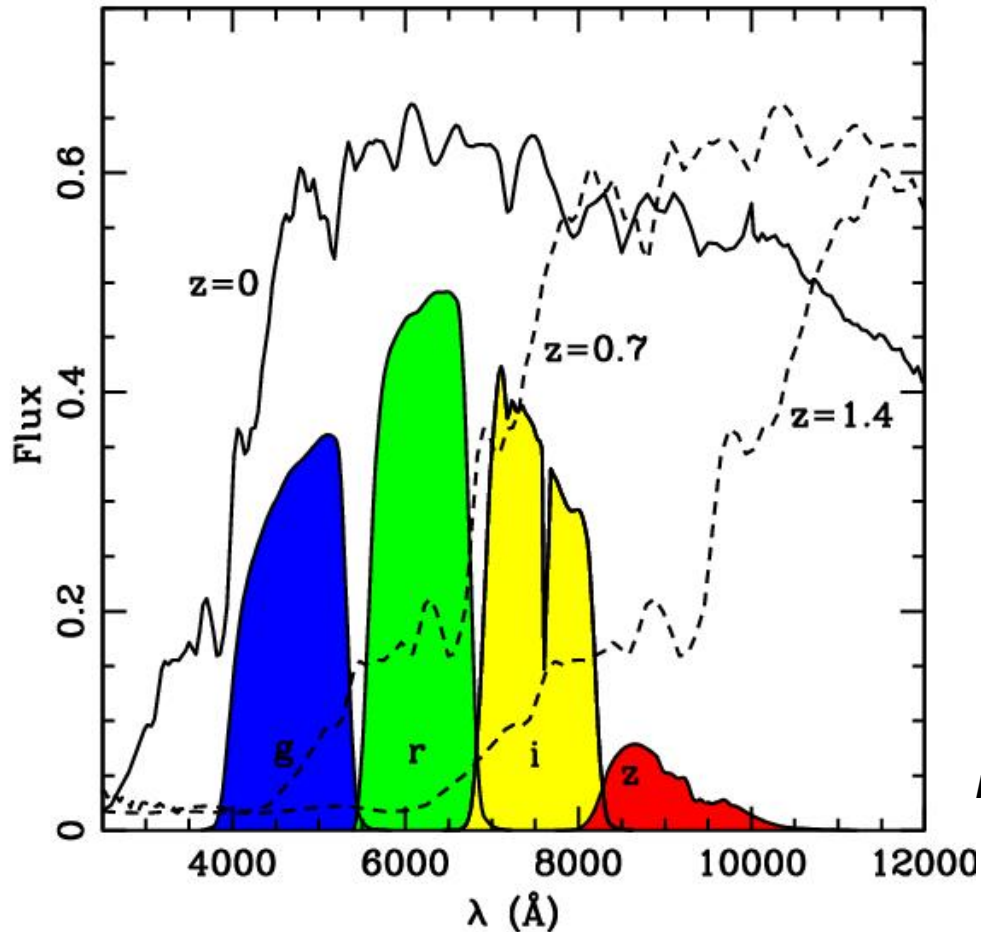
- **Photometric redshifts (photo-z's) are determined from the fluxes (or magnitudes or colors) of galaxies through a set of filters**
- **May be thought of as redshifts from (very) low-resolution spectroscopy**
- **Photo-z's are needed in particular when it's too observationally expensive to get spectroscopic redshifts (e.g., if galaxies are too many or too faint)**
- **Well-calibrated photo-z's are a key ingredient to obtaining cosmological constraints in large photometric surveys like DES and LSST**



Photometric Redshifts

DARK ENERGY
SURVEY

- The photo-z signal comes primarily from strong galaxy spectral features, like the 4000 Å break, as they redshift through the filter bandpasses

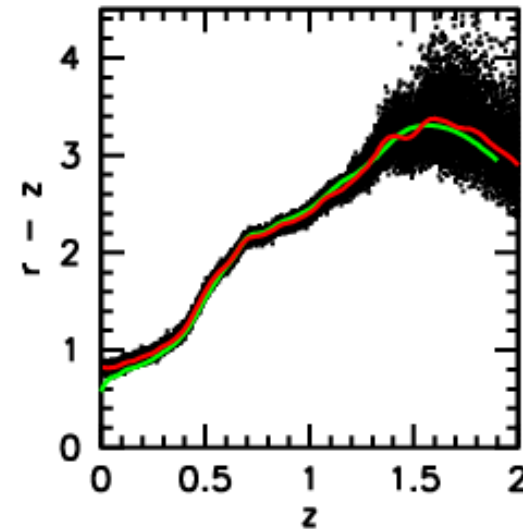
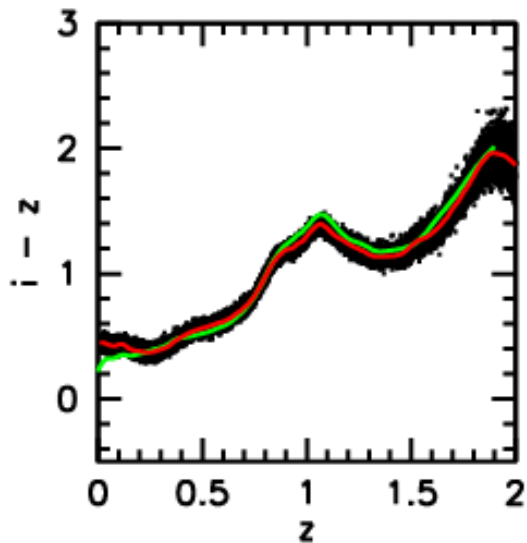
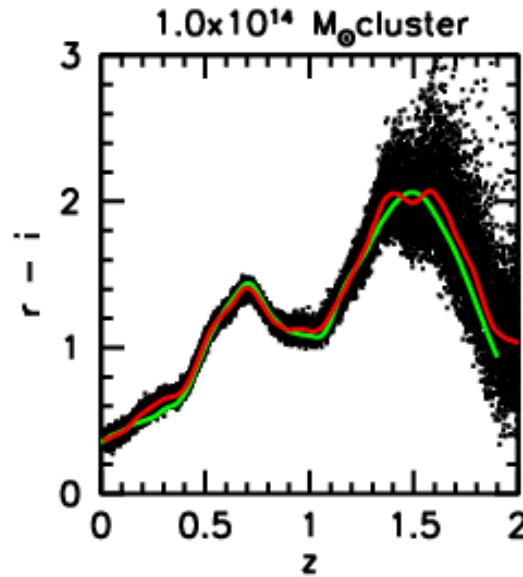
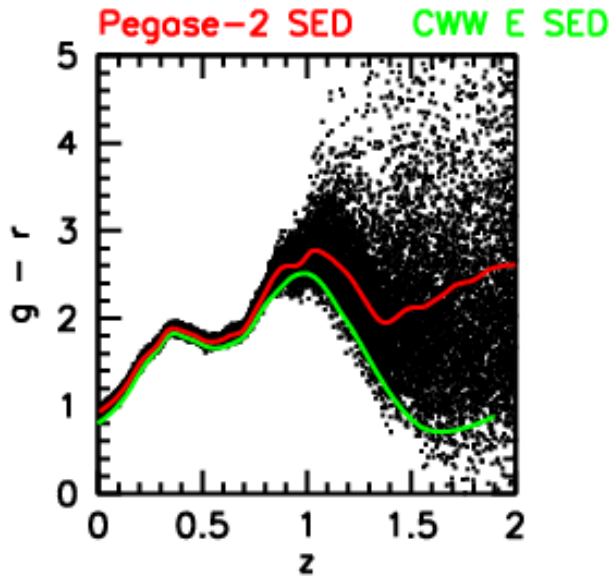


Early-type galaxy spectrum at three different redshifts ($z=0, 0.7, 1.4$) overlaid on SDSS griz filter throughputs

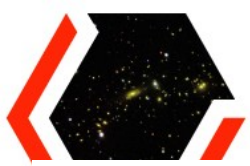
Figure from H. Oyaizu



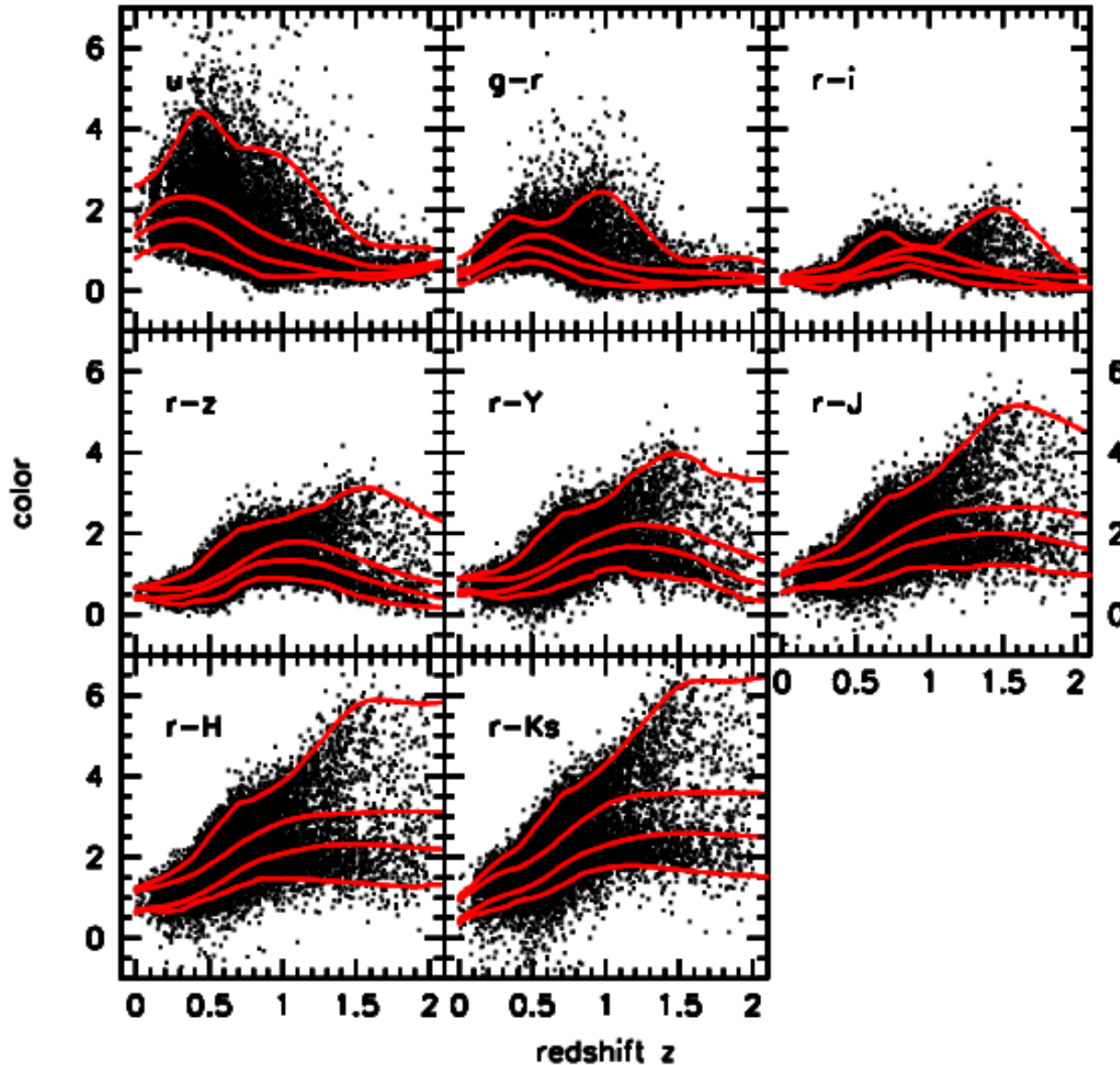
Cluster Galaxy Colors vs. Redshift



- *Simulated cluster galaxy colors (with noise) vs. redshift, based on one particular early-type galaxy spectral energy distribution (SED) evolution model (from “Pegase-2” library)*
- *From plotted color vs. redshift trends, one can see how the redshift (photo-z) may be inferred from the colors*



Galaxy Colors vs. Redshift

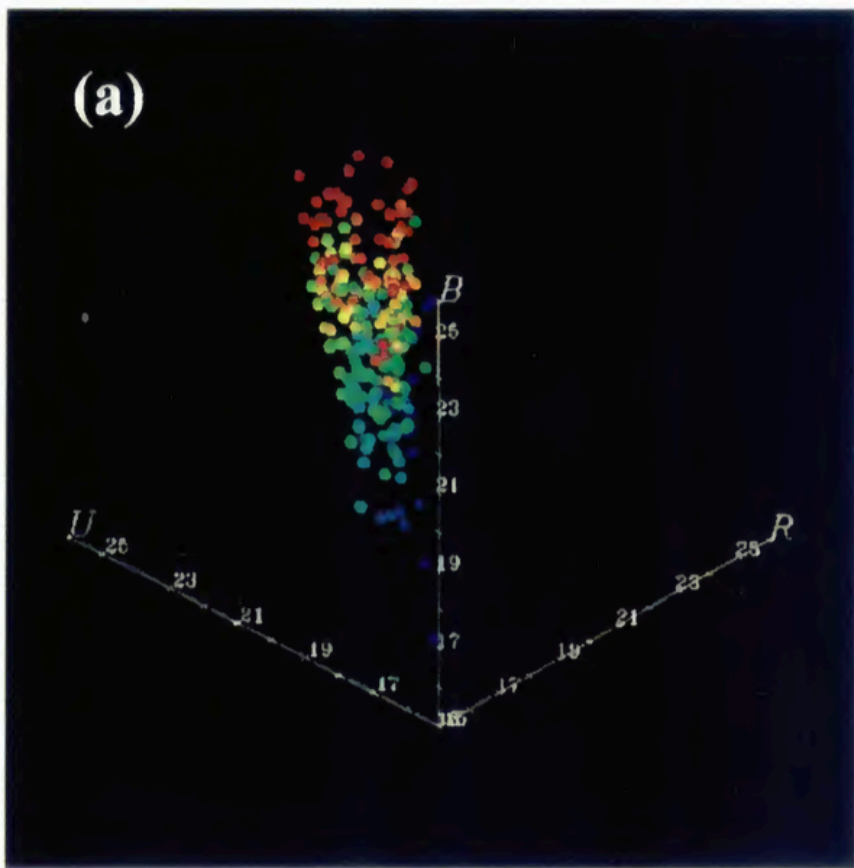


- *Simulated galaxy colors (with noise) vs. redshift from the “DES5yr” mock galaxy catalog*
- *A set of 4 empirical “CWW” (Coleman, Wu & Weedman 1980) SEDs (red curves) used to model the galaxy population*
- *Can see it’s harder to estimate photo-z’s when full galaxy population is present*



Slicing through multicolor space: Connolly et al. (1995)

Example showing how it is possible to disentangle redshifts from galaxy colors/magnitudes in multicolor space



=

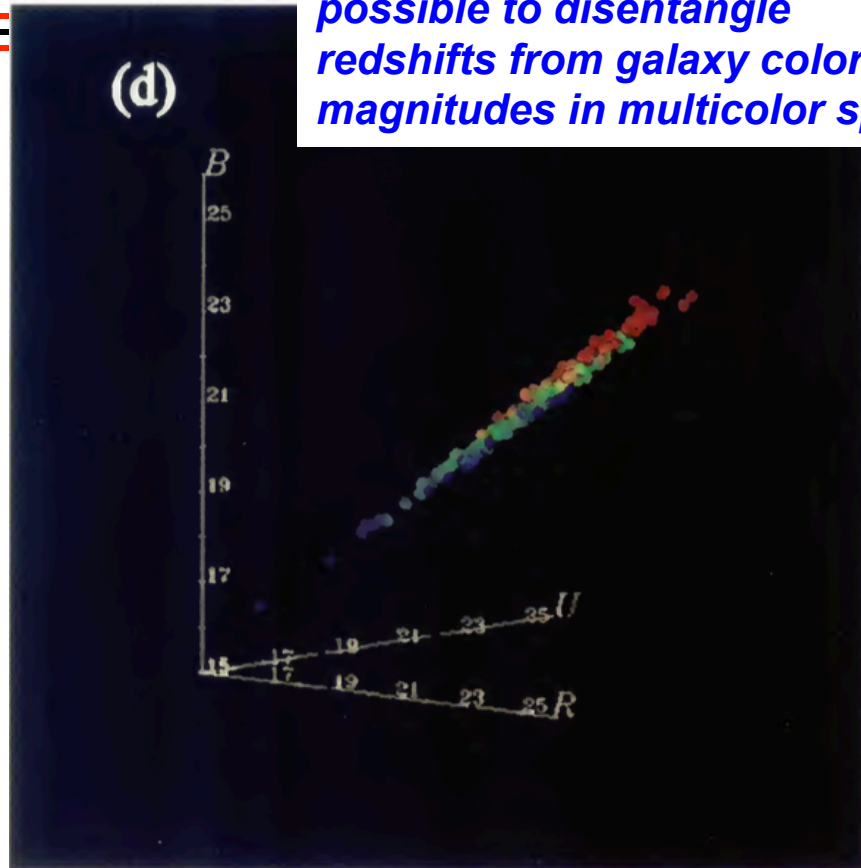


FIG. 1. The distribution of galaxies within the three-color space U , B_J , and R_F is shown for the sample of galaxies derived from the spectroscopic redshift surveys of Koo & Kron. The redshift of each galaxy is encoded by the color of its data point, blue corresponds to $z=0$ and red to $z=0.5$. The color table is set so that each color maps onto an interval of 0.1 in redshift. Panels (a), (b), and (d) show three orthogonal perspectives of the data. Panel (c) shows a schematic of the distribution. The position of a galaxy within the three-color space is determined by its redshift, luminosity, and spectral type. For a given redshift the data form thick slabs in the UB_JR_F space. Redshifting the galaxies moves these slabs through the color space (due to dimming and K corrections).



Photo-z Methods

- **Two basic categories**
 - **Machine learning/training set/empirical methods**
 - **Template-fitting methods**
- **For lists of methods, see, e.g.,**
 - **Hildebrandt et al. (2010): “PHAT: Photo-z Accuracy Testing”**
 - **Zheng & Zhang (2012) SPIE review (<http://adsabs.harvard.edu/abs/2012SPIE.8451E..34Z>)**
 - **Sanchez et al. (2014): DES Science Verification (SV) photo-z comparison testing; later slides**



Photo-z Methods

- ***Machine learning/training set/empirical methods***
 - Use “training set” to derive a relation between redshift and magnitudes/ fluxes/colors/etc.
 - May also output $p(z)$, the full redshift probability distribution function (PDF), in addition to “point” estimates
 - Rely on training set, which can often be incomplete/unrepresentative of full photometric data
 - Simple examples:
 - Polynomial fit (Connolly et al. 1995)
 - Neural networks (Collister & Lahav 2004)



Photo-z Methods

- **Example: quadratic polynomial fit (e.g. Connolly et al. 1995)**
 - **Adopt a quadratic polynomial relation between redshift z and magnitudes g,r,i**

$$\begin{aligned} z = & a_0 + a_1 * g + a_2 * r + a_3 * i \\ & + a_4 * g*g + a_5 * r*r + a_6 * i*i \\ & + a_7 * g*r + a_8 * g*i + a_9 * r*i \end{aligned}$$

- **Derive best-fit polynomial coefficients $a_0, a_1, a_2, \dots, a_9$ from training set data with spectroscopic redshifts**
- **Photo-z's then come from applying best-fit relation to photometric data**
- **Training set and photometric data should be observed by the same telescope/instrument/filters, ideally under the same conditions (exposure time, seeing, etc.)**



Photo-z Methods

DARK ENERGY
SURVEY

- **Example: artificial neural network (from Oyaizu et al. 2008)**

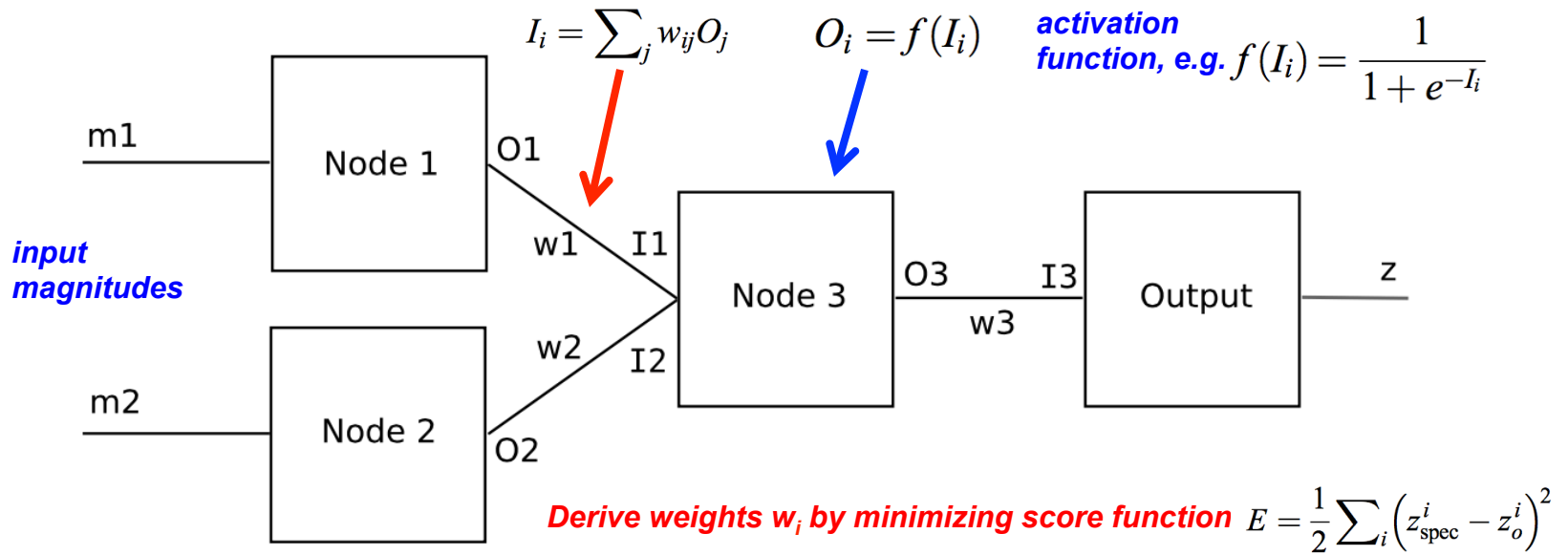


FIG. 3.— Simple FFMP network with three layers and configuration 2:1:1. The inputs are the two magnitudes, m_1 and m_2 . I_x denotes the input from node x , and O_x is the corresponding output of this node. The weights w associated with each connection are found by training the network using training and validation sets (see text).

- **The neural network here is really just a complex function of the input magnitudes**
- **To avoid “overfitting,” minimization steps are done on training set but final set of weights are chosen to be those that perform best on independent “validation set”**
- **Multiple networks may also be examined to optimize photo-z solution**



Photo-z Methods

- ***Template-fitting methods***
 - Use a set of SED templates (from real data or from models)
 - Calculate fluxes/magnitudes using redshifted templates and filter throughputs
 - Obtain best-fitting galaxy redshift and template type, and also $p(z)$
 - Rely on template library, which may not fully span the range of galaxy types in photometric sample
 - Examples:
 - HyperZ (Bolzonella et al. 2000)
 - BPZ (Benitez 2000, Coe et al. 2006)
 - LePhare (Arnouts et al. 2002, Ilbert et al. 2006)

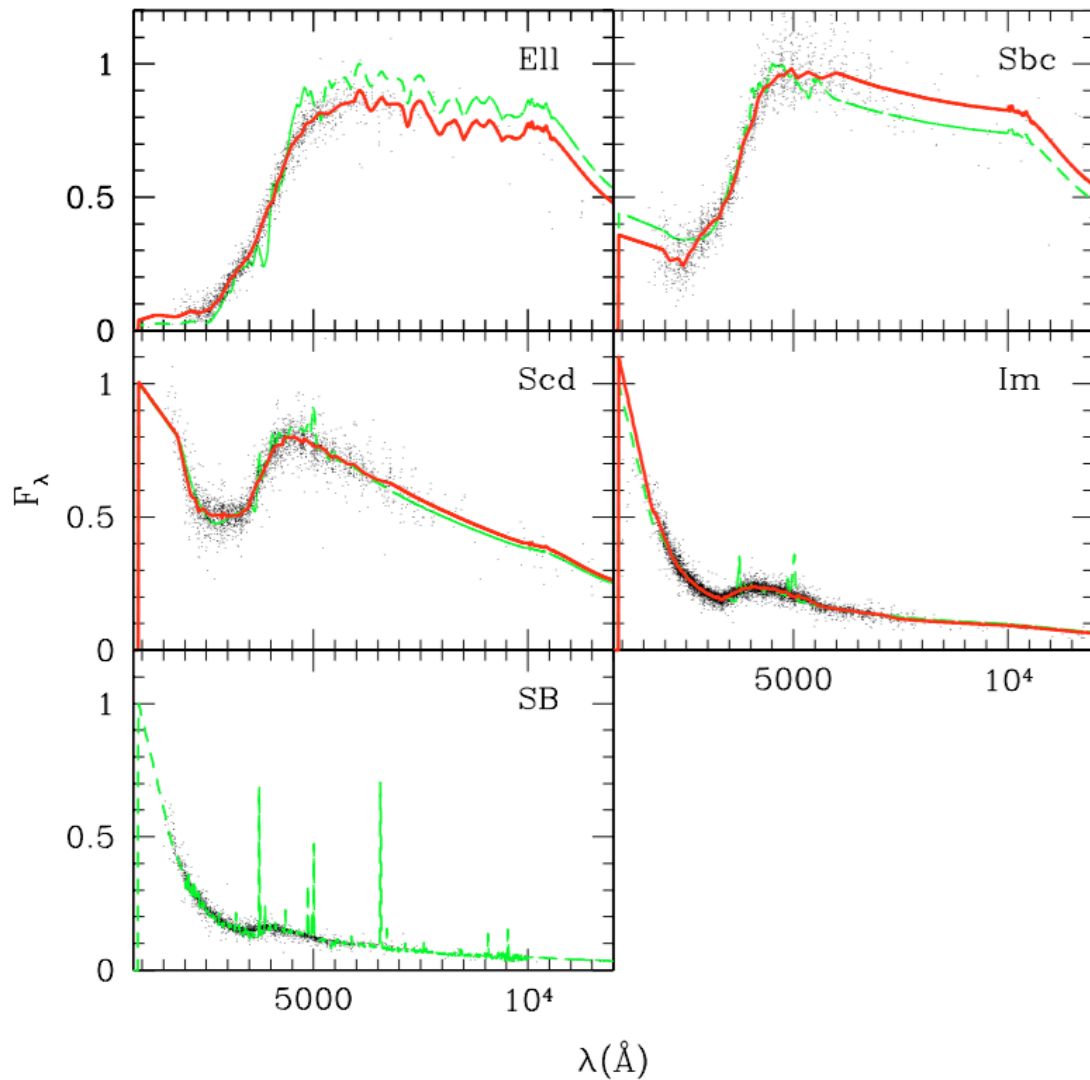


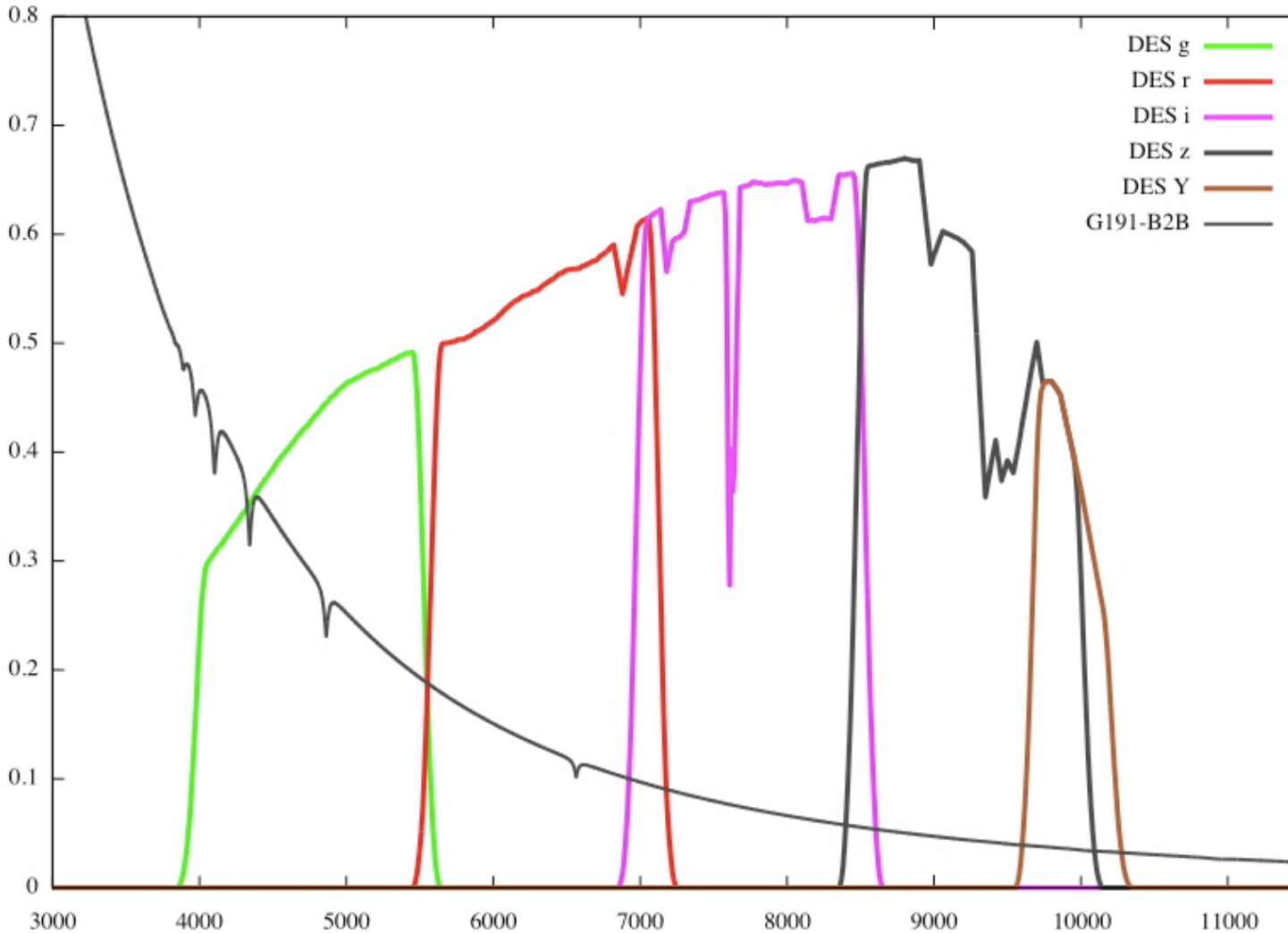
Fig. 5. Each panel corresponds to one of the four CWW templates (Ell, Sbc, Scd, Irr) and one starburst template (Kinney et al. 1996). The points correspond to the flux of each galaxy redshifted to the rest-frame using the spectroscopic redshifts. The green dashed lines are the initial SEDs and the red solid lines are the optimised SEDs which are the output of the procedure described in Sect. 4.2. The starburst template is not optimised.

- **Example of galaxy template library based on real data**
- **Use of a small number of templates (with interpolation between them), can give “ok” photo-z’s**

Ilbert et al. (2006)



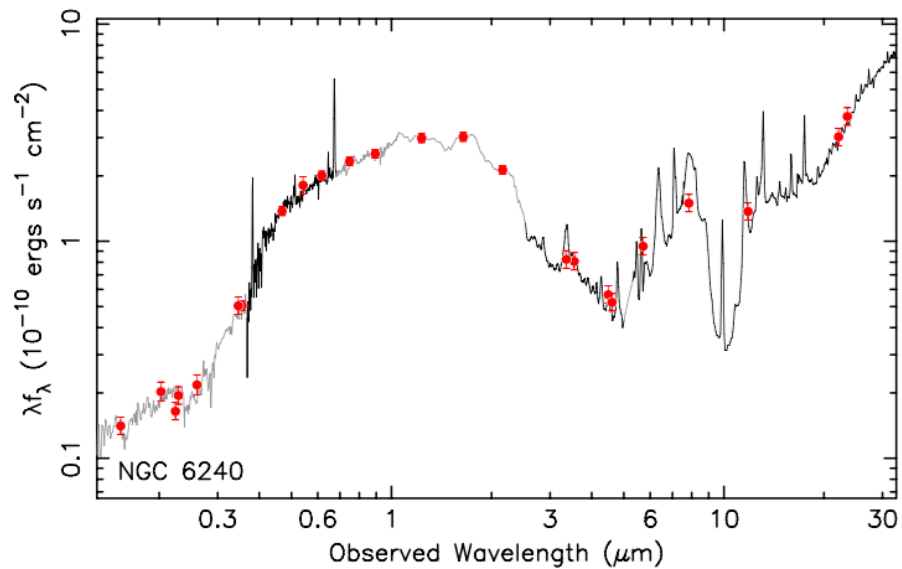
**DARK ENERGY
SURVEY**



- **DES throughput curves, including atmosphere, telescope, DECam optics, filters, and CCDs**

- **Need to be accurately measured for use in template fitting photo-z methods**

*From Douglas
Tucker*



Example UV to IR SED from a more modern galaxy SED atlas (Brown et al. 2014)

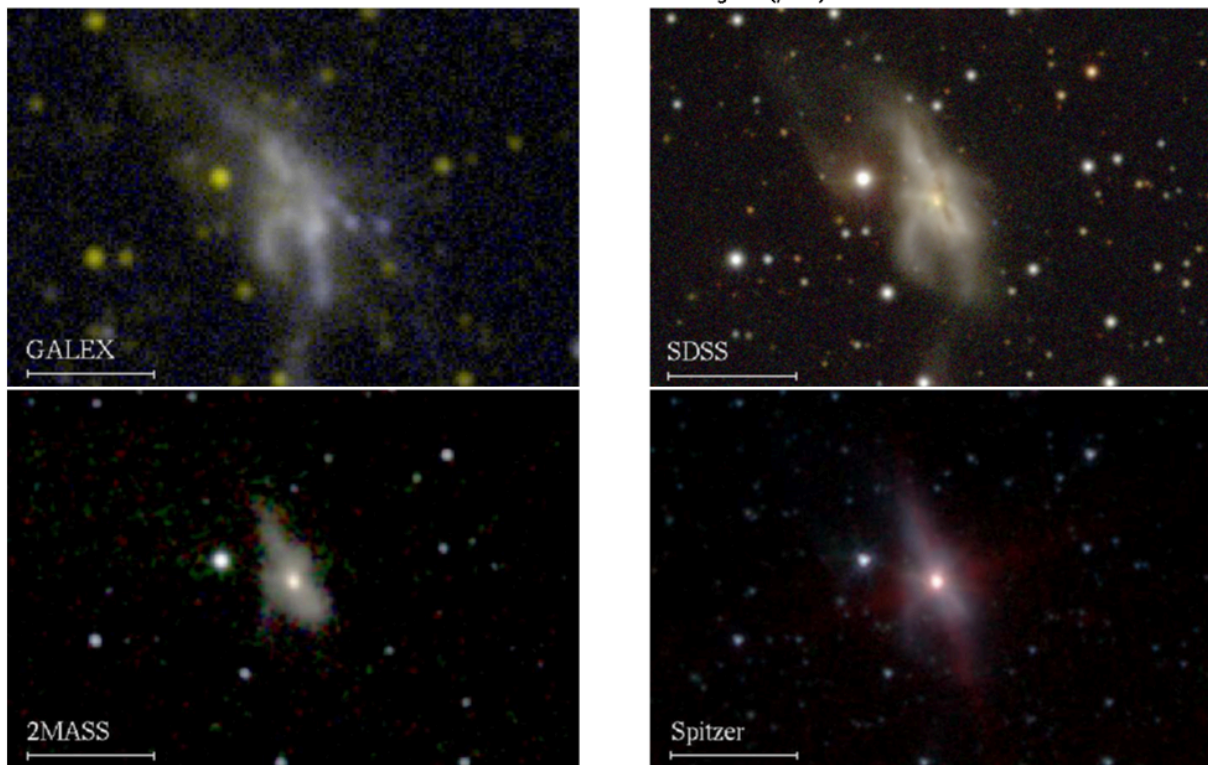


Figure 1. Ultraviolet to mid-infrared SED of NGC 6240 (top panel), along with some of the *GALEX*, *SDSS*, *2MASS*, and *Spitzer* images that were used to constrain and verify the SED. The horizontal bar denotes an angular scale of 1'. In the top panel, the observed and model spectra are shown in black and gray respectively, while the photometry used to constrain and verify the spectra is shown with red dots.

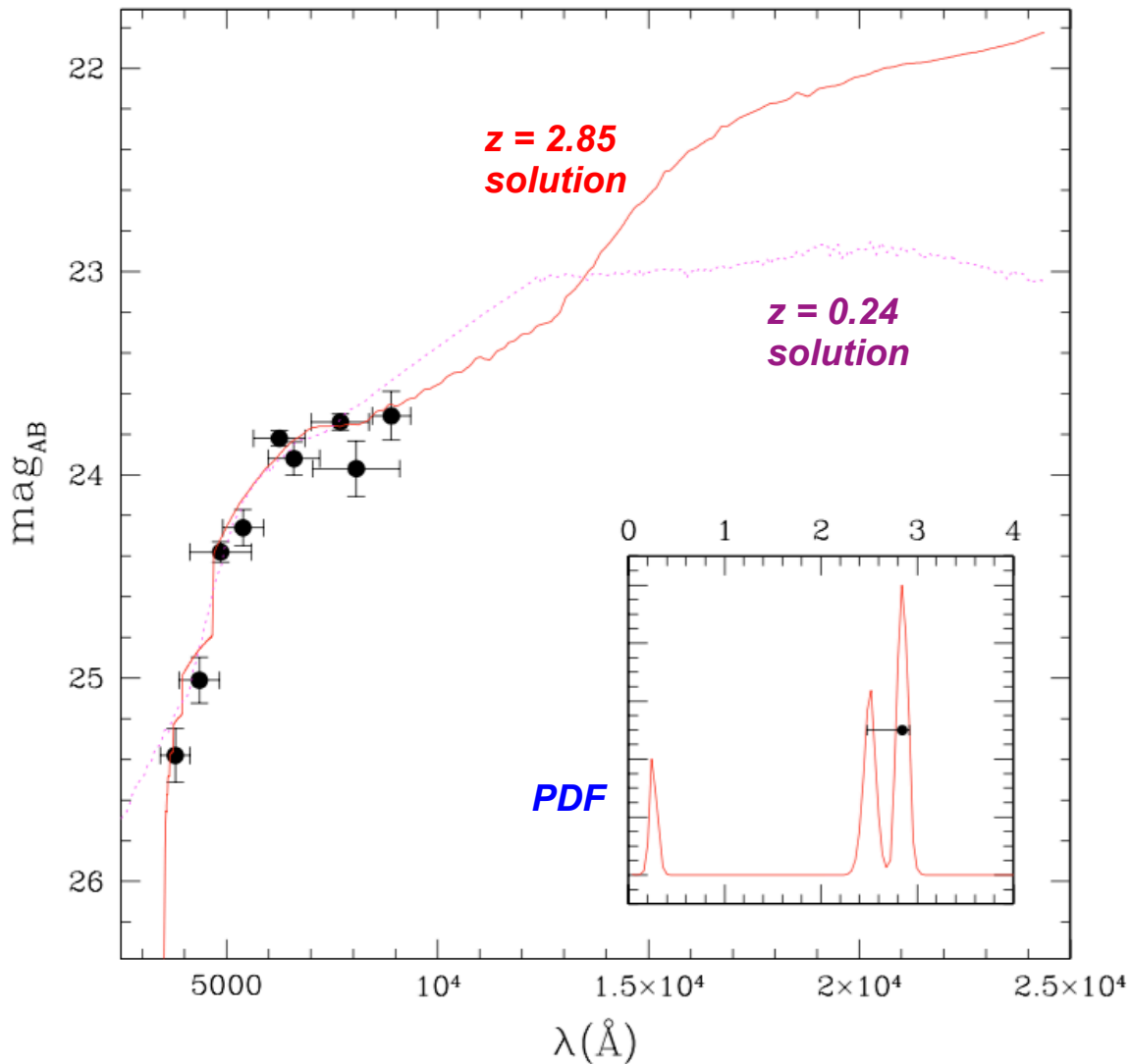


Fig.4. Example of best-fitted templates on multi-colour data for a galaxy at $z_s = 0.334$. The solid black points correspond to the apparent magnitudes in the u^* , B , g' , V , r' , R , i' , I , z' filters from the left to right respectively. The solid line corresponds to a template redshifted at $z_p = 2.85$ and the dotted line at $z_p = 0.24$. The enclosed panel is the associated Probability Distribution Function (PDFz).

- **Illustration of template fitting method**
- **True redshift is $z=0.334$**
- **Also shows confusion between low redshift “Balmer break” and high redshift “Lyman break” features (at about 5000\AA observed wavelength)**
- **Degeneracy can be broken with more data (here, more IR data) or by using priors (see next slides)**

Ilbert et al. (2006)



Photo-z Methods

- **Example: Bayesian photometric redshifts (BPZ; Benitez 2000)**
 - **Bayes' Theorem (redshift z , colors C , magnitudes m_0 , types T)**

$$p(z | C, m_0) = \frac{p(z | m_0)p(C | z)}{p(C)} \propto p(z | m_0)p(C | z)$$

posterior (blue arrow pointing to $p(z | C, m_0)$)

prior (purple arrow pointing to $p(z | m_0)$)

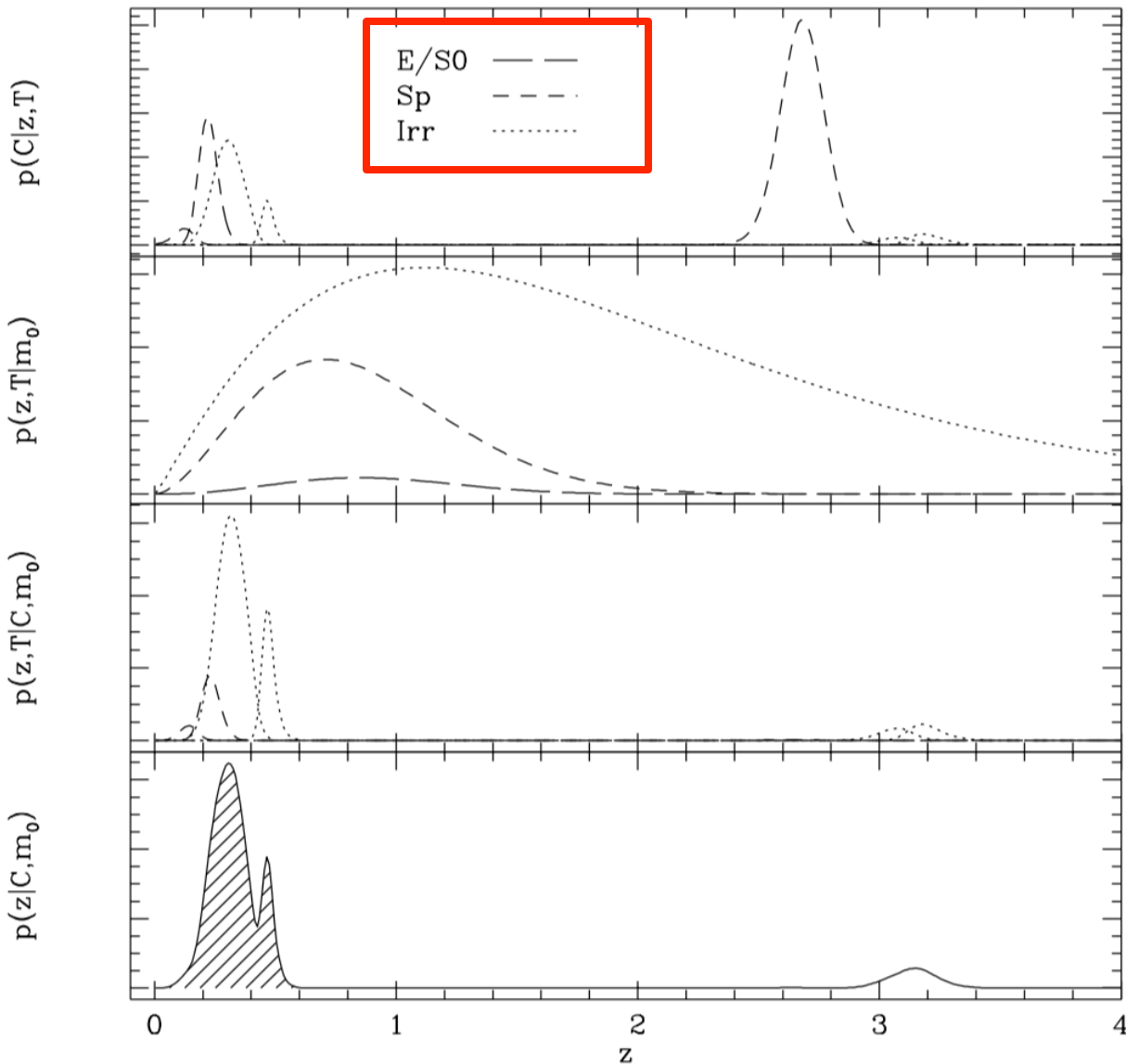
likelihood (red arrow pointing to $p(C | z)$)

- **Sum over posterior probability distributions for different galaxy types to get final redshift PDF**

$$p(z | C, m_0) = \sum_T p(z, T | C, m_0) \propto \sum_T p(z, T | m_0)p(C | z, T)$$

- **Using a flat (i.e., constant) prior is the same as maximum likelihood**

likelihoods



priors

posteriors

final,
summed
probability

Benitez (2000)

FIG. 2.—Example of the main probability distributions involved in BPZ for a galaxy at $z = 0.28$ with an Irr spectral type and $I \approx 26$, to which random photometric noise is added. From top to bottom: (a): Likelihood functions $p(C|z, T)$ for the different templates used in § 4. Based on ML, the redshift chosen for this galaxy would be $z_{\text{ML}} = 2.685$, and its spectral type would correspond to a spiral. (b): Prior probabilities, $p(z, T|m_0)$, for each of the spectral types (see text). Note that the probability of finding a spiral spectral type with $z > 2.5$ and a magnitude $I = 26$ is almost negligible. (c) Probability distributions, $p(z, T|C, m_0) \propto p(z, T|m_0)p(C|z, T)$, that is, the likelihoods in the top plot multiplied by the priors. The high-redshift peak due to the spiral has disappeared, although there is still a small chance of the galaxy being at high redshift if it has a Irr spectrum, but the main concentration of probability is now at low redshift. (d) Final Bayesian probability, $p(z|C, m_0) = \sum_T p(z, T|C, m_0)$, which has its maximum at $z_b = 0.305$. The shaded area corresponds to the value of $p_{\Delta z}$, which estimates the reliability of z_b and yields a value of ≈ 0.91 .



DES photometric redshifts

DARK ENERGY
SURVEY

- **DES will rely on photometric redshifts (photo-z's), i.e., redshifts determined from photometric imaging data, in primarily the 5 DES filters grizY (plus u band and near-IR JHK as available)**
- **Well understood photo-z's and photo-z errors are vital for deriving accurate cosmology constraints from the different DES dark energy probes**
- **Large and deep samples of galaxies with spectroscopic redshifts and/or highly precise photo-z's, combined with DES photometry, are used to train and calibrate (validate) DES photo-z measurements**



DES Science Verification (SV) spectroscopic redshift training set fields

DARK ENERGY
SURVEY

- **ugrizY** imaging was obtained during DES Science Verification (SV; Nov 2012 – Feb 2013) on 4 fields with deep spectroscopic redshift training set data
- **VVDS Deep 02hr** (in DES supernova X3 deep field)
 - VVDS Deep redshift sample to $I_{AB} < 24$
- **CDFS** (in DES supernova C3 deep field)
 - VVDS Deep redshift sample to $I_{AB} < 24$
 - ACES redshift sample to $i < \approx 23$
 - OzDES Deep redshift sample to $i < 21$
- **VVDS Wide 14hr**
 - VVDS Wide redshift sample to $I_{AB} < 22.5$
- **COSMOS** (courtesy of DECam community program, PI A. Dey)
 - zCOSMOS Bright redshift sample to $I_{AB} < 22.5$
 - VVDS Wide 10hr redshift sample to $I_{AB} < 22.5$
- Plus additional bright redshift samples in above fields from **SDSS-I/II, SDSS-III/BOSS, and 2dFGRS**



Photo-z comparison tests on DES SV data: Standardized redshift samples

DARK ENERGY
SURVEY

- **Goal to compare, test, and optimize photo-z codes used in the DES Photo-z Working Group**
- **“Standardized” training and validation galaxy redshift data sets assembled for use by all codes**
 - **“Main”**: DES main survey depth photometry
 - **5859 (training set) + 6381 (validation set) high-confidence redshifts**
 - **“Deep”**: typically 3x exposure of single supernova deep field visit
 - **7249 (training set) + 8358 (validation set) high-confidence redshifts**
- **Standardized set of DECam system throughput curves also assembled for use**



Photo-z comparison tests on DES SV data: Training sets

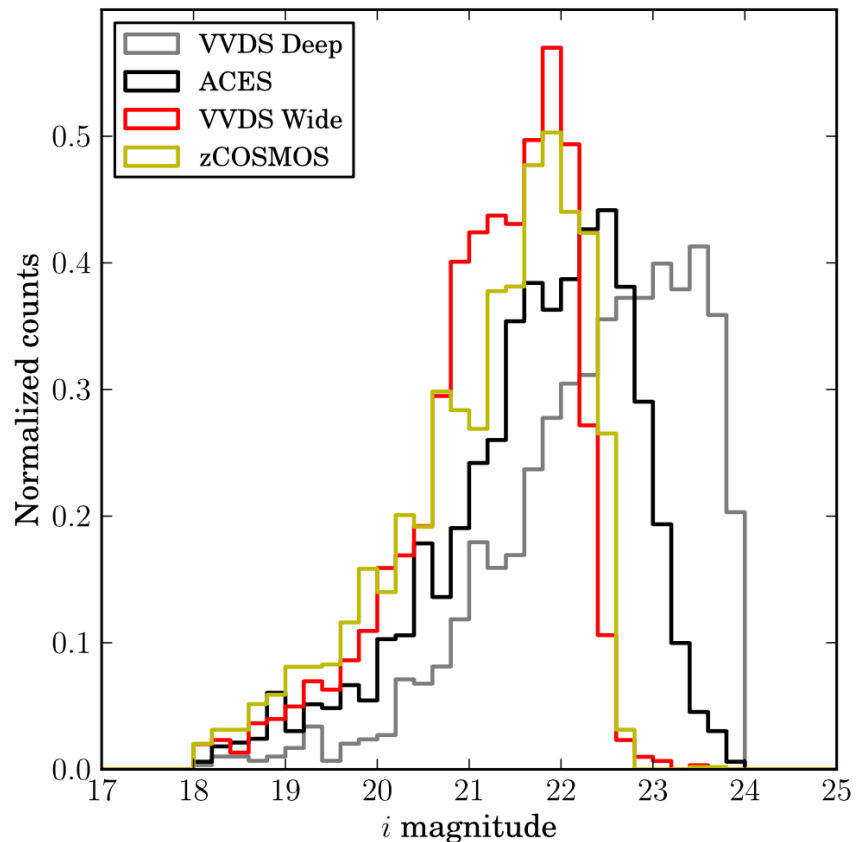


Figure 19. *i*-band magnitude distributions for the four training samples used in Test 4, each corresponding only to one of the four major spectroscopic samples used, one from each of the calibration fields.

Primary SV training sets

Sanchez et al. (2014)

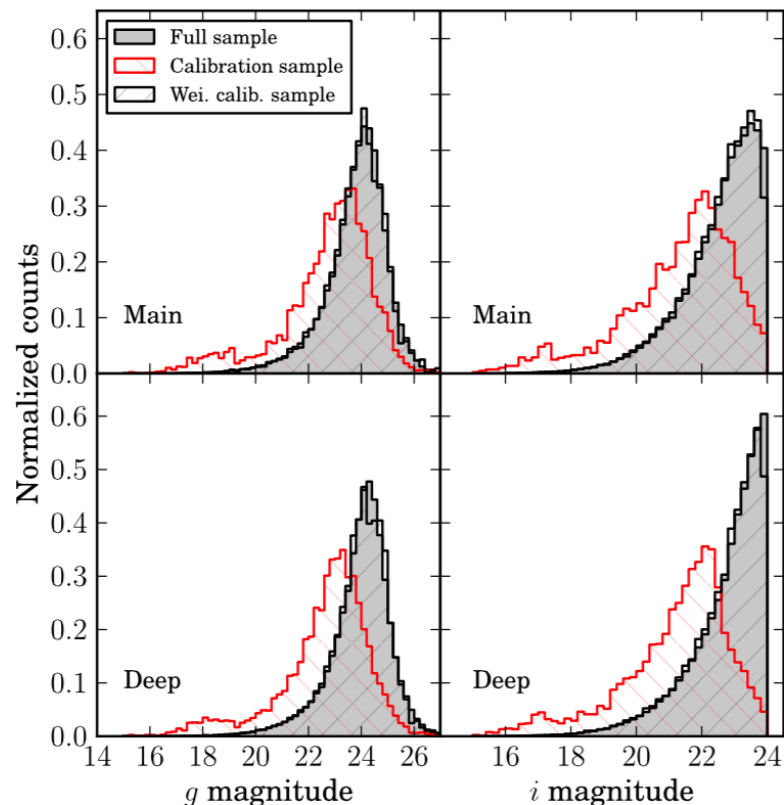


Figure 4. *g*- and *i*-magnitude distributions for the full, calibration and weighted calibration sample. The difference between the full and the calibration samples is apparent, the latter being significantly brighter. After applying the weighting procedure described in Lima et al. (2008), the weighted calibration distributions agree very well with the corresponding DES-SV distributions.

Spectroscopic data weighted to match photometric sample



Photo-z comparison tests on DES SV data: Photo-z codes

DARK ENERGY
SURVEY

Table 3. List of methods used to estimate photo-z's. Code type and main references are given.

Code	Type	Reference
DESDM, artificial neural network	Training based	Oyaizu et al. (2008a)
ANNZ, artificial neural network	Training based	Collister & Lahav (2004)
TPZ, prediction trees and random forest	Training based	Carrasco Kind & Brunner (2013, 2014)
RVMZ, relevance vector machine	Training based	Tipping (2001)
NIP-KNNZ, normalized inner product nearest neighbor	Training based	de Vicente et al., in preparation
ANNZ2, machine-learning methods	Training based	Sadeh et al., in preparation
ARBORZ, boosted decision trees	Training based	Gerdes et al. (2010)
SKYNET, classification artificial neural network	Training based	Bonnett (2013) and Graff et al. (2013)
BPZ, Bayesian photometric redshifts	Template based	Benitez (2000) and Coe et al. (2006)
EAZY, easy and accurate redshifts from Yale	Template based	Brammer et al. (2008)
LEPHARE	Template based	Arnouts et al. (2002) and Ilbert et al. (2006)
ZEBRA, Zurich extragalactic Bayesian redshift analyzer	Template based	Feldmann et al. (2006)
PHOTOZ	Template based	Bender et al. (2001)

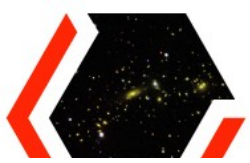
Sanchez et al. (2014)



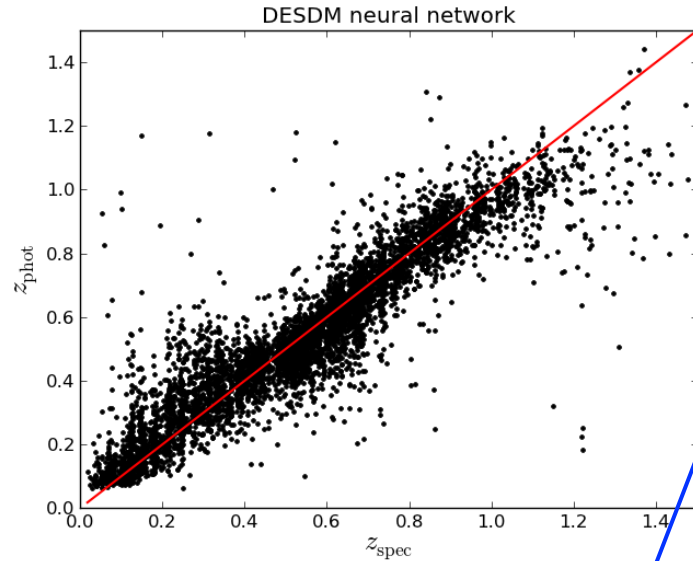
Photo-z comparison tests on DES SV data: Comparison test metrics

DARK ENERGY
SURVEY

- **Comparison tests of photo-z codes based on a set of metrics, primarily the following (with DES science requirements in parentheses):**
 - **Mean bias $z(\text{phot}) - z(\text{spec})$**
 - **Scatter σ and σ_{68} (< 0.12)**
 - **2σ ($< 10\%$) and 3σ ($< 1.5\%$) outlier fractions**
 - **Bias and σ of $z(\text{phot}) - z(\text{spec})$ normalized by the photo-z error**
 - **N_{Poisson} : rms difference between photo-z and true z distributions, normalized by Poisson fluctuations**
- **Metrics applied after culling 10% of galaxies in each method with largest photo-z errors, per science requirements**
- **Metrics also weighted to account for incompleteness of redshift samples, in order to be appropriate for an $i < 24$ DES galaxy sample**



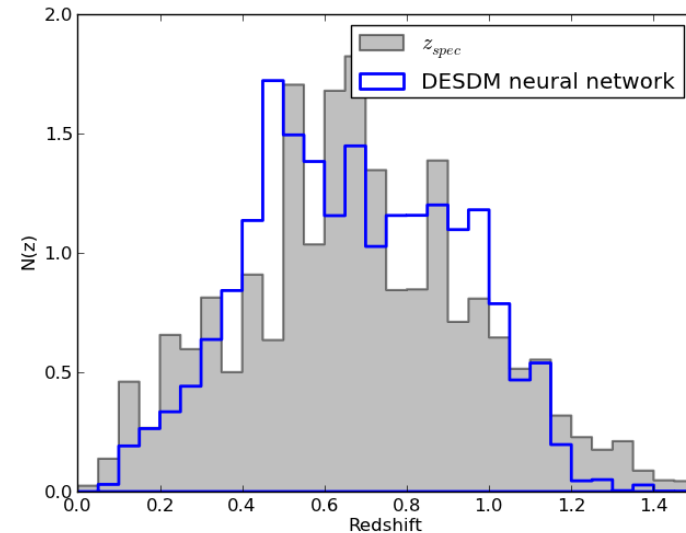
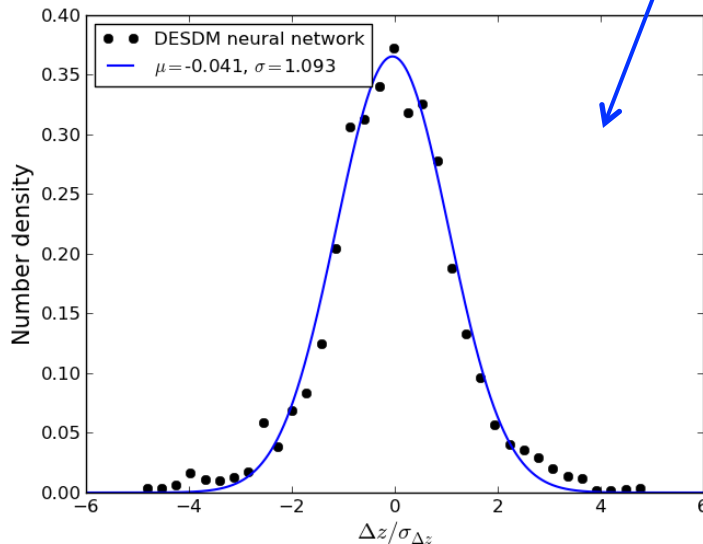
Example photo-z results, for DESDM neural network method



←
Top left: Photo-z vs. spectro-z

Bottom left: Photo-z – spectro-z, normalized by photo-z errors, and Gaussian fit

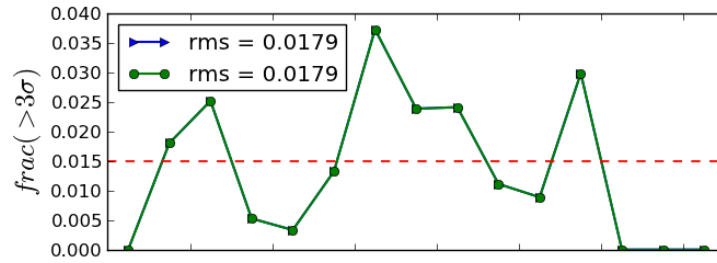
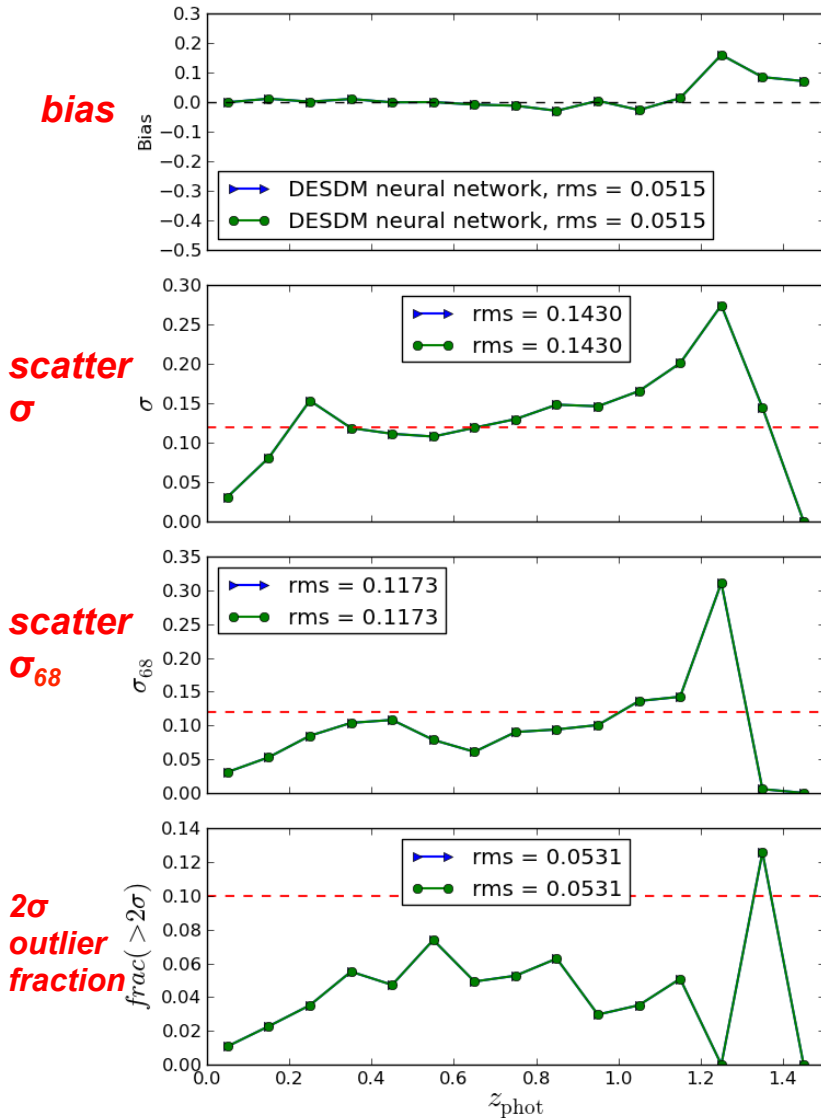
Bottom right: Photo-z redshift distribution compared to true redshift distribution



**Plots generated
using Python code
of M. Carrasco**



Example photo-z statistics, for DESDM neural network method



**3 σ
outlier
fraction**



All statistics plotted vs. photo-z, in bins of redshift width = 0.1

Plots generated using Python code of M. Carrasco

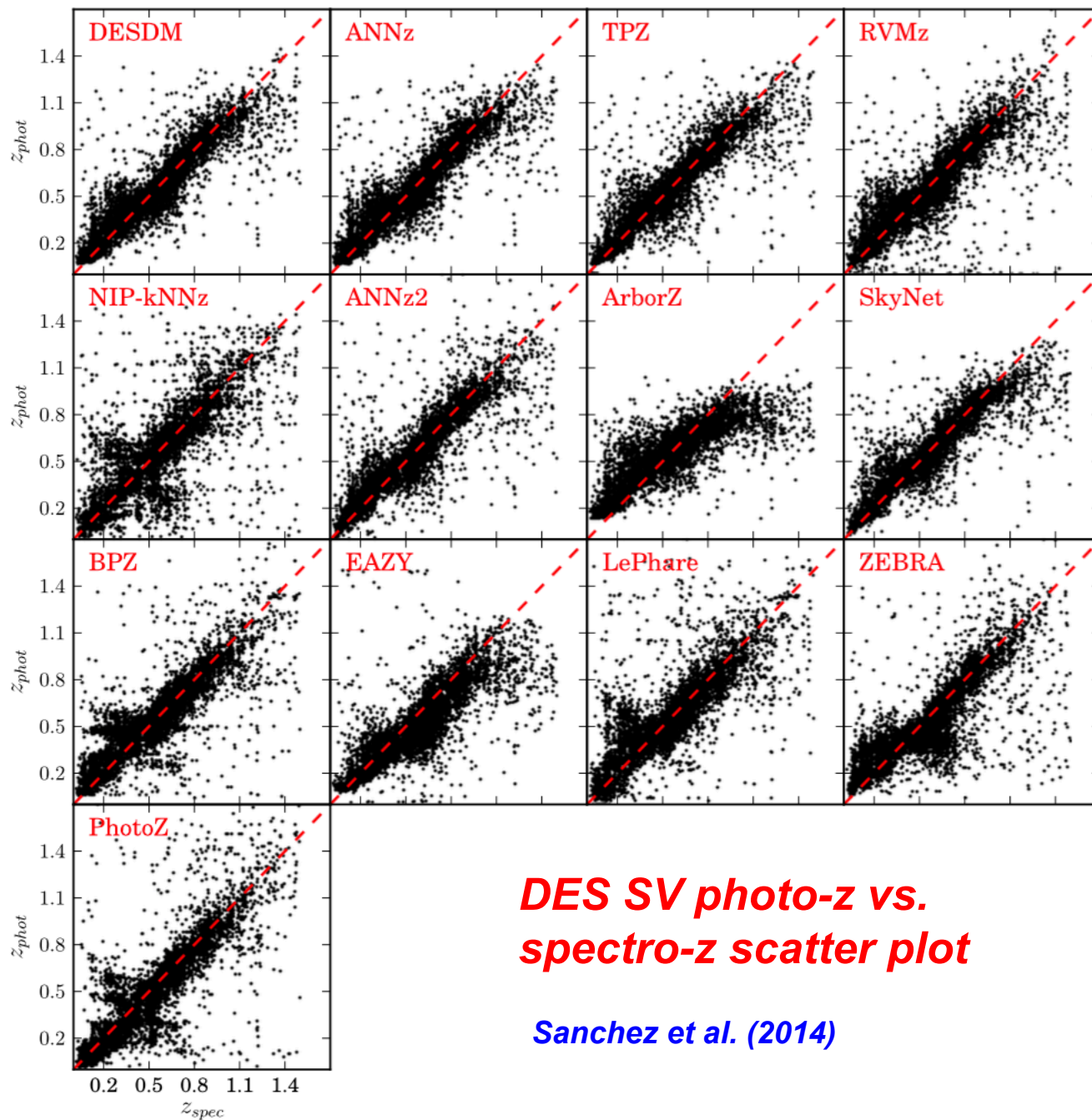
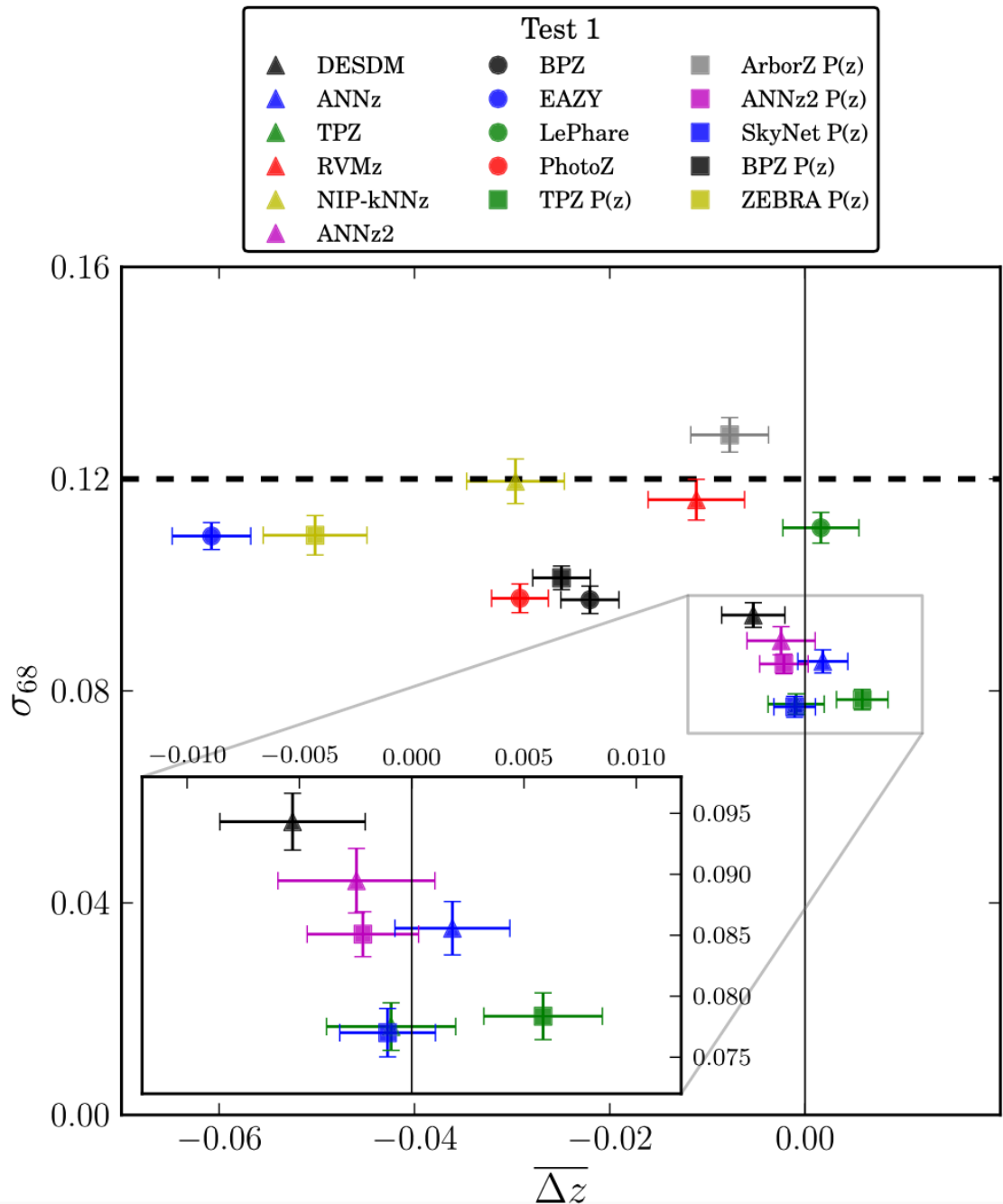


Figure 5. z_{phot} versus z_{spec} scatter plot for all the codes analysed in Test 1 and listed in Table 3.



***DES SV photo-z
σ₆₈ vs. bias plot***

Sanchez et al. (2014)

Figure 6. σ_{68} versus bias for all the codes analysed in Test 1. The black



Photo-z comparison tests on DES SV data: Summary of results

DARK ENERGY
SURVEY

- **Most methods meet DES photo-z scatter requirement $\sigma_{68} < 0.12$**
- **All methods meet requirement that 2σ outlier fraction $< 10\%$, and a few methods also meet 3σ outlier fraction $< 1.5\%$, though most methods are close at $< 2\%$**
- **However, challenge is meeting requirement on uncertainty of photo-z bias and scatter**



Photo-z calibration errors and dark energy constraints

DARK ENERGY
SURVEY

Dark energy constraint degradation < 10% for photo-z bias/scatter uncertainty in 0.001-0.01 range
Requires training set of 10^4 - 10^5 spectroscopic redshifts (Ma, Hu, & Huterer 2006)

Weak Lensing Tomography

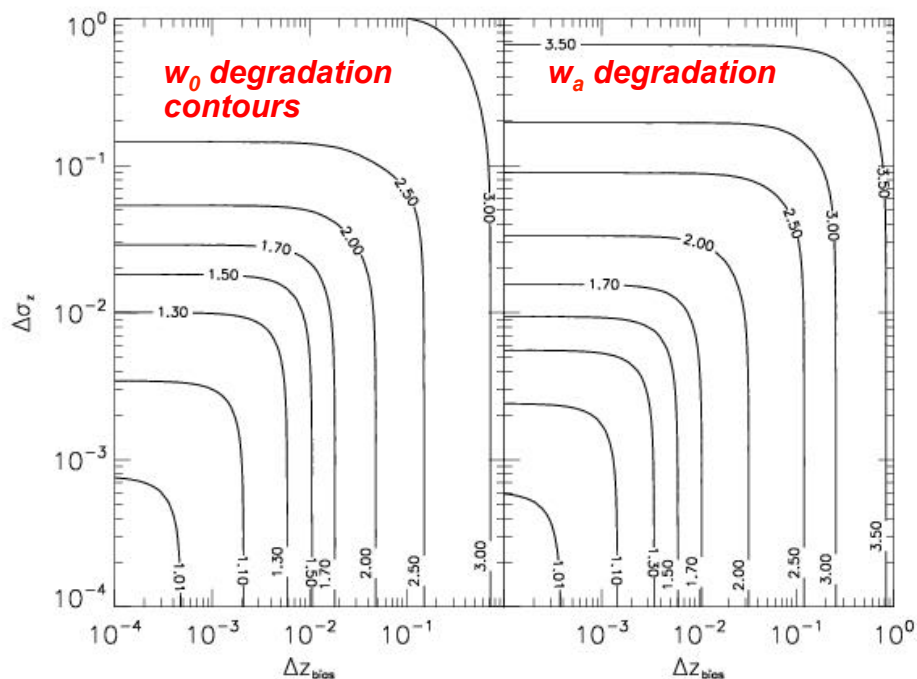
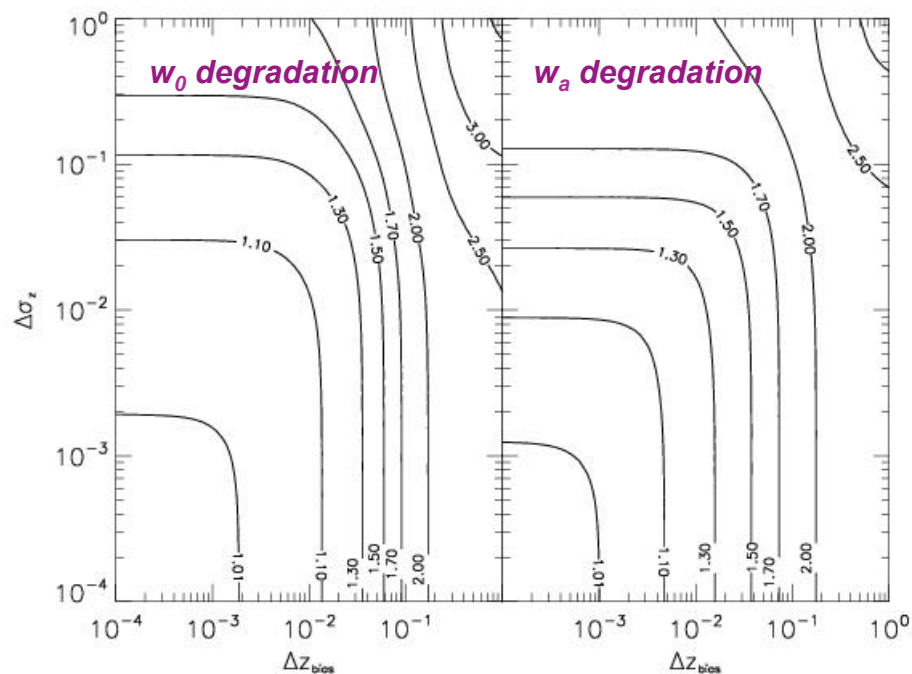


photo-z bias(x-axis) or scatter(y-axis) uncertainties

Baryon Acoustic Oscillations



(from Z. Ma)



Photo-z calibration challenges

DARK ENERGY
SURVEY

- See Newman et al. (2013) Snowmass report
- For dark energy constraints, we typically want to know the uncertainty in the mean redshift (within a “tomographic” (photo-z) redshift bin) at the level of

$$\Delta(\langle z \rangle) \sim 0.002 (1+z)$$

- Naively, given photo-z’s with $\sigma_z = 0.1$ (like DES), and $N=10000$ spectroscopic redshifts, we we would get

$$\Delta(\langle z \rangle) = \sigma_z / \sqrt{N} = 0.001$$

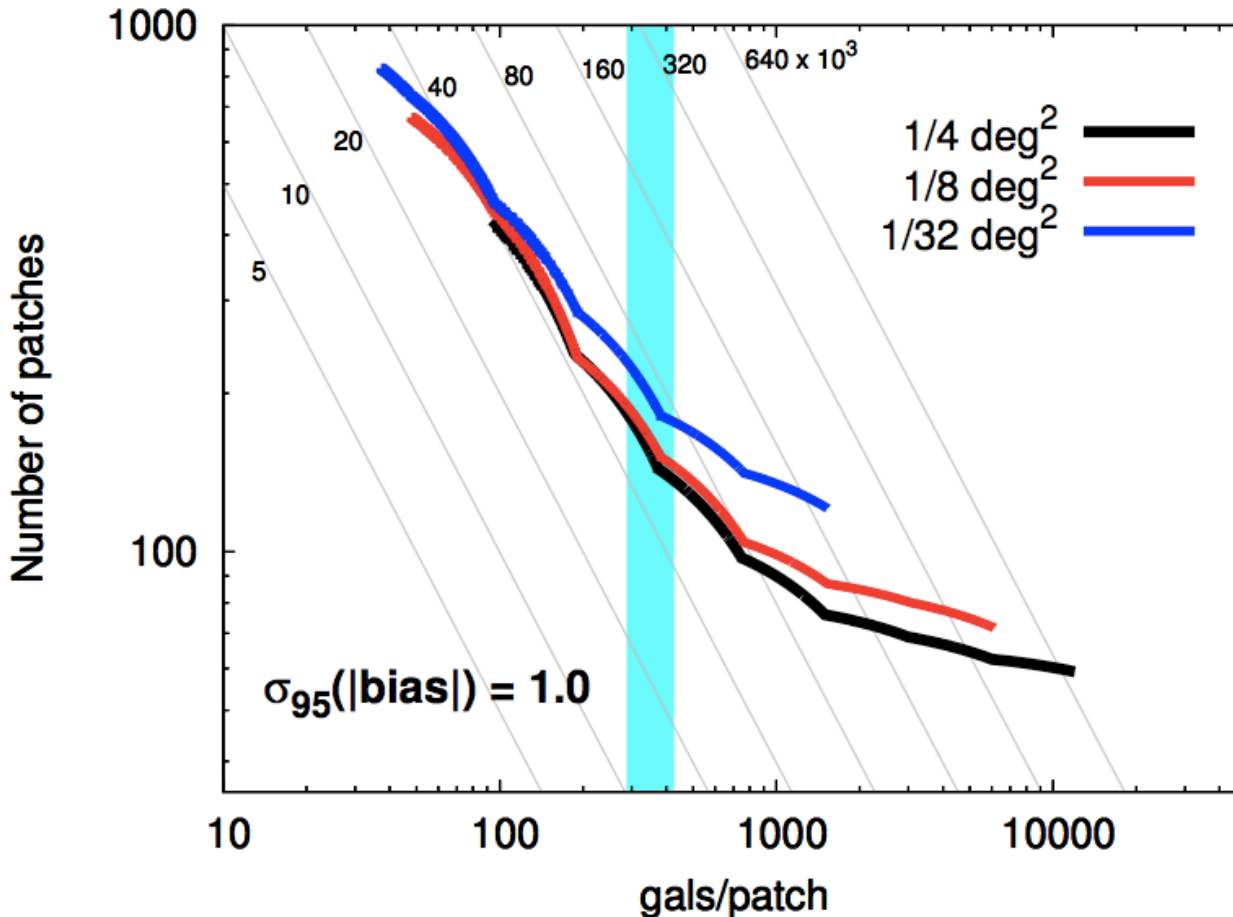
- However, this neglects the important challenges of
 - **Cosmic variance** (also called sample variance) due to large scale structure
 - **Incompleteness** of spectroscopic samples



Cosmic variance (or sample variance)

DARK ENERGY
SURVEY

Sample variance requirements (Cunha et al. 2012) on spectro-z sample to calibrate photo-z's, for weak lensing shear measurements of w



- *Need 150 Magellan/IMACS-sized patches, well separated on the sky*
- *About 400 galaxies observed per patch*
- *4 hour exposures, completeness like that of the VIMOS-VLT Deep Survey (VVDS) (assuming random failures)*
- *Need about 75 nights of Magellan time*



Cosmic variance (or sample variance)

DARK ENERGY
SURVEY

- **Cunha et al. (2012) analysis is “direct,” “brute-force” calibration**
- **There may be mitigation strategies possible (see Newman et al. 2013, p. 16) that reduce the requirements**
- **Newman et al. (2013) quote the requirements instead as**
 - **~30000 redshifts, over $>\sim 15$ widely separated fields, each ~ 0.1 deg in size**
 - **Their Table 2-2 show more detailed observing estimates, still quite substantial**
- **However, systematic incompleteness needs to be at $<\sim 0.1\%$ for direct calibration purposes**
- **Such a sample is more likely to be used to meet training set requirements**



Spectroscopic incompleteness

DARK ENERGY
SURVEY

- **Unlike SDSS at low redshifts/bright magnitudes, spectroscopic redshift samples at higher redshifts/fainter magnitudes (e.g., to $i = 24$ for DES) are incomplete (Newman et al. 2013 quote a 30-60% “secure” redshift failure rate for deep spectro-z surveys)**
- **We can correct for incompleteness by weighting in magnitude/color space as we did for the SV testing, but this assumes the incompleteness can be fully captured in observable properties like color and magnitude**
- **For example, perhaps there is some hidden incompleteness as a function of true redshift that remains even after weighting**



DES photo-z calibration/validation for weak lensing shear analysis

DARK ENERGY
SURVEY

- For DES SV weak lensing shear analysis, despite spectroscopic incompleteness we nonetheless used weighted spectroscopic samples to estimate an uncertainty $\Delta(\langle z \rangle) \sim 0.05$ in the mean redshift for the tomographic (photo-z) redshift bins used for the analysis (see Bonnett et al. 2016)
- The SV uncertainties were comparable to statistical uncertainties and cosmic variance and were good enough for the SV-sized sample
- For Y1 analysis we will need to improve to $\Delta(\langle z \rangle) \sim 0.02$ and will instead
 - Use highly-precise photo-z samples, which are also presumably much more complete, for validation
 - Also incorporate “cross-correlation redshifts” to estimate redshift distributions $N(z)$ and to validate photo-z’s



DES SV weighted spectroscopic training and validation data, used for weak lensing shear analysis

TABLE I. The number of galaxies that are included in the matched spectroscopic catalogue are listed for each spectroscopic survey with the corresponding mean redshift and mean i band magnitude. Further details can be found in Appendix A.

Spectroscopic survey	Count	Mean i	Mean z
VIPERS	7286	21.52	0.69
GAMA	7276	18.61	0.22
Zcosmos	5442	20.93	0.51
VVDS F02 Deep	4381	22.40	0.68
SDSS	4140	18.82	0.39
ACES	3677	21.73	0.58
VVDS F14	3603	20.61	0.49
OzDES	3573	19.85	0.47
ELG cosmos	1278	22.22	1.08
SNLS	857	21.09	0.55
UDS VIMOS	774	22.54	0.85
2dFGRS	725	17.52	0.13
ATLAS	722	18.96	0.35
VVDS spF10 WIDE	661	21.16	0.53
VVDS CDFS DEEP	544	22.05	0.62
UDS FORS2	311	23.80	1.25
PanSTARRS MMT	297	19.94	0.35
VVDS Ultra DEEP	264	23.71	0.88
PanSTARRS AAOmega	239	19.69	0.32
SNLS AAOmega	81	21.16	0.56

Bonnett et al. (2016)

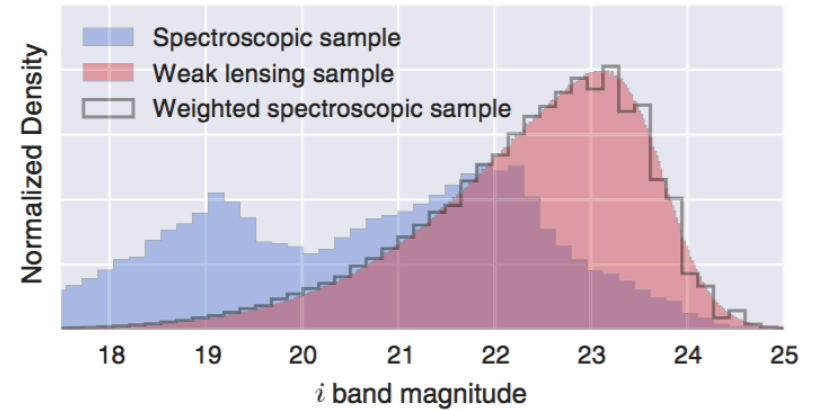


FIG. 5. The i -band magnitude distribution of the matched spectroscopic catalogue is shown in blue and the weak lensing sample is shown in red. The matched spectroscopic catalogue after weighting is shown as the grey histogram outline overlaying the weak lensing sample.



DES SV $N(z)$ and mean redshifts in tomographic bins, used for weak lensing shear analysis

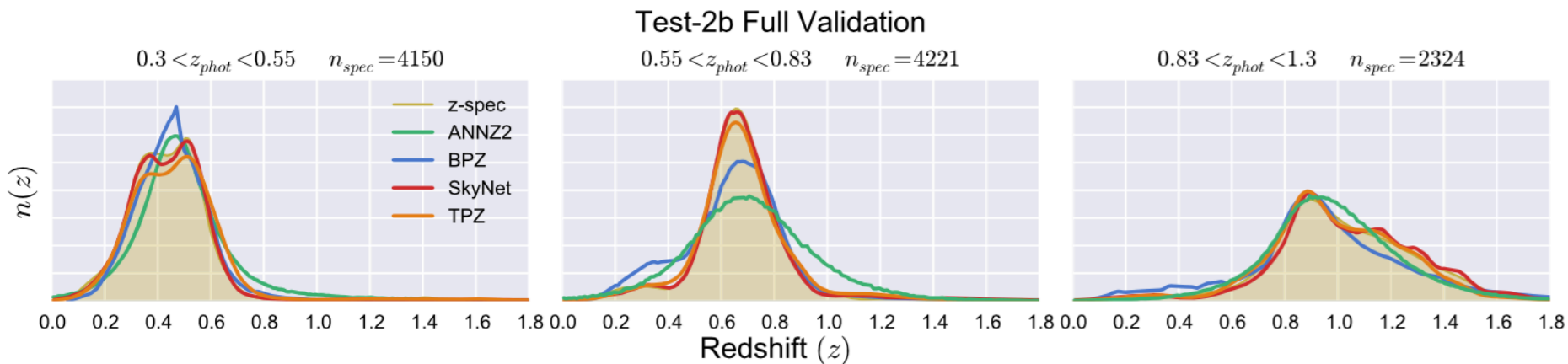
DARK ENERGY SURVEY

TABLE IV. The estimated mean of the three tomographic bins in the NGMIX sample of the four photo- z methods and the estimate of the weighted spectroscopic sample.

z range	Spec (weighted)	ANNZ2	BPZ	SKYNET	TPZ
0.30–0.55	0.45	0.49	0.46	0.45	0.46
0.55–0.83	0.67	0.69	0.64	0.67	0.67
0.83–1.30	1.00	0.98	0.97	1.02	1.01

Estimate $\Delta(\langle z \rangle) \sim 0.05$ in tomographic bins

Bonnett et al. (2016)





Many-band photo-z samples for validation of DES photo-z's

DARK ENERGY
SURVEY

- **COSMOS 30-band (Laigle et al. 2016)**
 - Reaches DES depth, $dz/(1+z) \sim 0.007$
 - Overlaps deep DES SV/community data
- **ALHAMBRA 23-band (Molino et al. 2014)**
 - reaches DES depth, $dz/(1+z) \sim 0.01-0.014$
 - Alhambra-4/COSMOS (0.25 deg^2): overlaps deep DES SV/community data
 - Alhambra-2/DEEP2 (0.5 deg^2): in DES Y3 footprint, could be done to full depth in Y4
 - Alhambra-8/SDSS (0.5 deg^2): \sim full depth already obtained in Y4

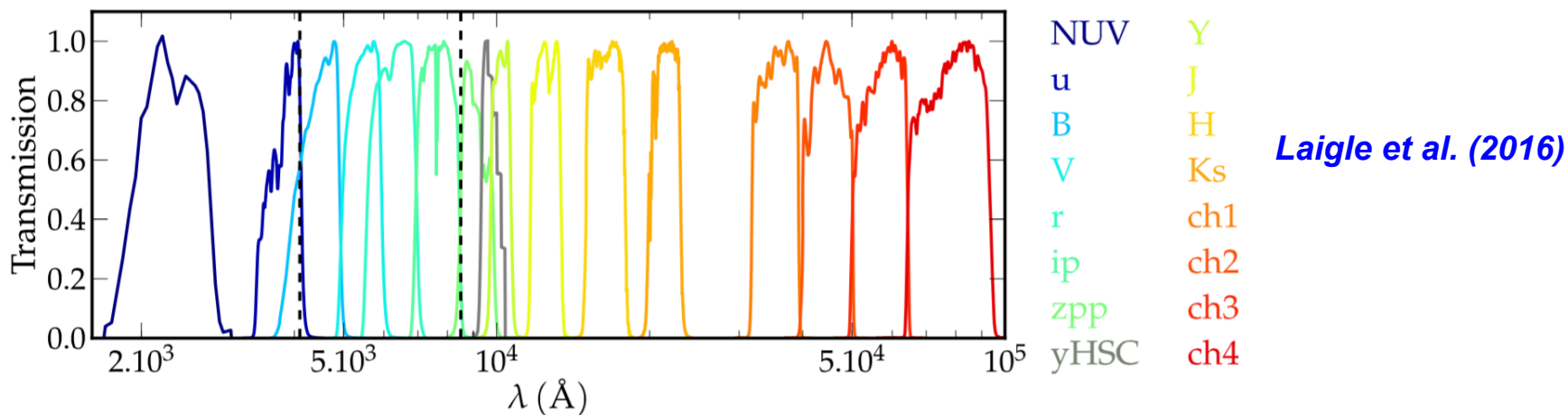
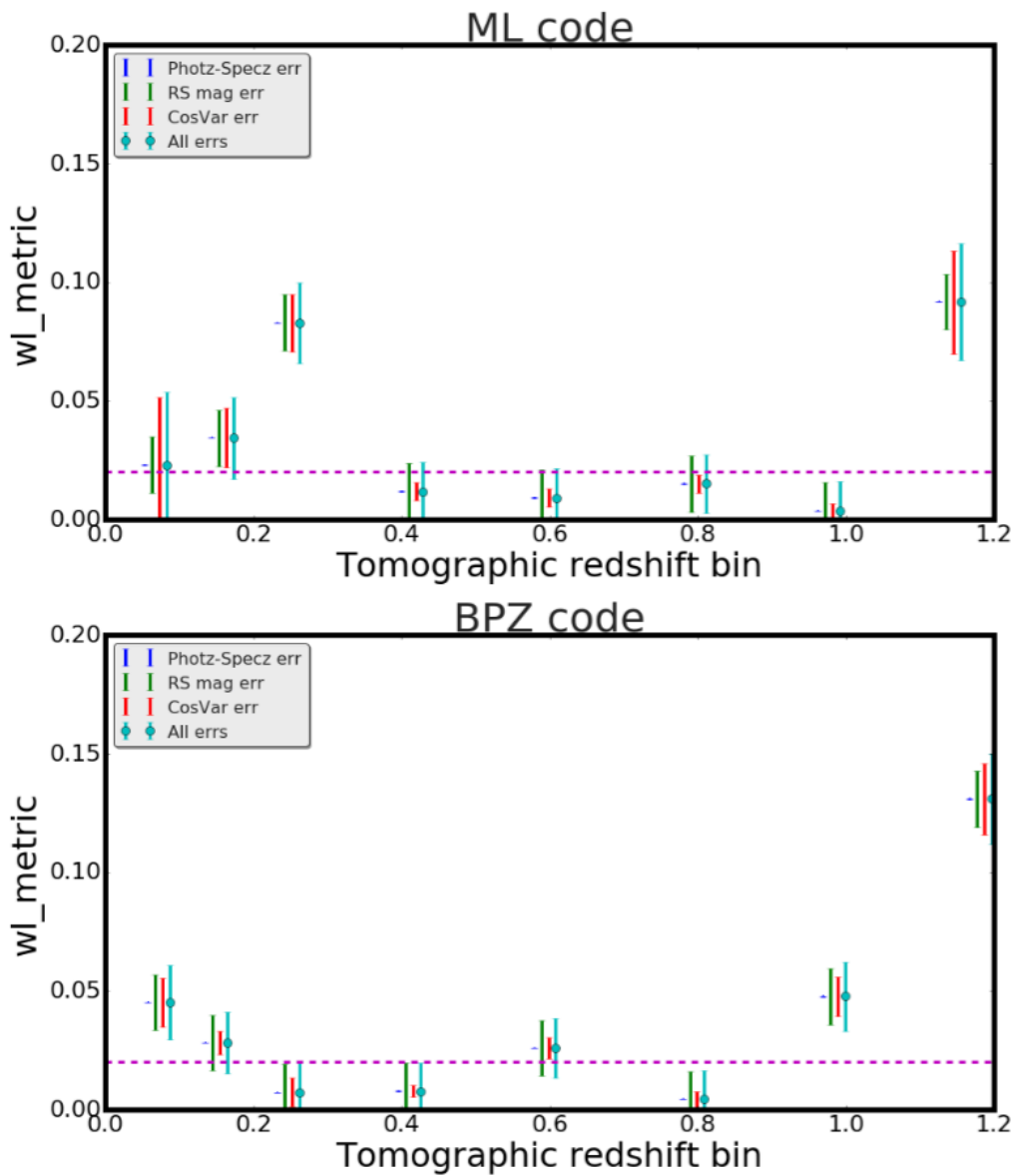


Figure 2. Transmission curves for the photometric bands used. The effect of atmosphere, telescope, camera optics, filter, and detector are included. Note that for clarity the profiles are normalized to a maximum throughput of one; therefore, the relative efficiencies of each telescope and detector system are *not* shown. Intermediate and narrow bands are not represented, but the region of the spectrum covered by these bands is marked by dashed lines.



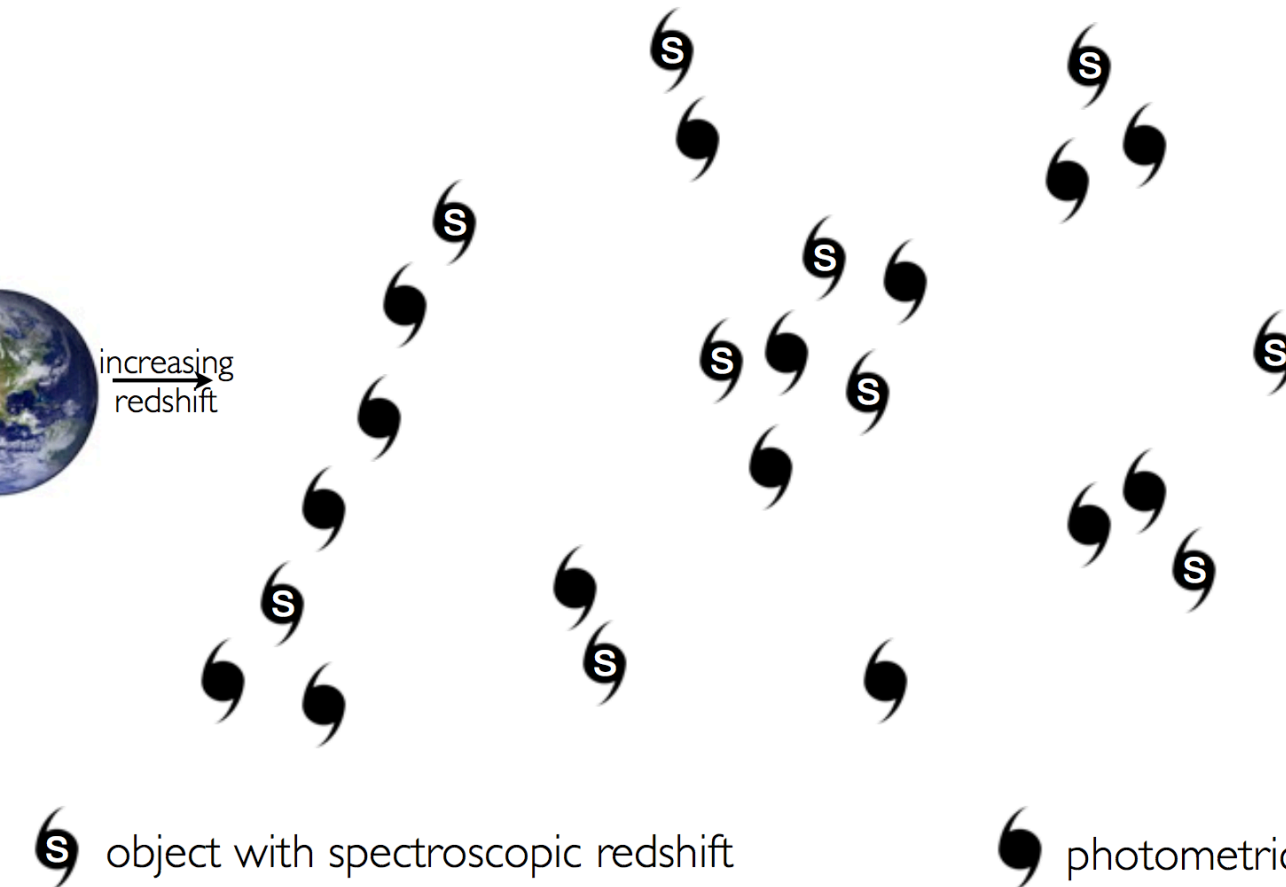
**Current, preliminary
DES Y1 validation
results for weak
lensing mean
redshift bias metric,
from B. Hoyle**

Figure 8: The top (bottom) panel shows the final weak lensing metric ($| \langle z_{true} \rangle - \langle z_{desphot} \rangle |$) values calculated using ML (BPZ) redshift routine. The error bars include both sample variance and magnitude re-sampled error components. The green dotted line shows the requirements on this metric value from the weak lensing group.



Cross-Correlation Redshifts

DARK ENERGY
SURVEY



- *Galaxies are correlated with each other, i.e., more likely to find a neighboring galaxy compared to random distribution*
- *Characterized by spatial (ξ) or angular (w) correlation functions*
- *Expect non-zero correlations between galaxies only if they are close in redshift (neglecting lensing magnification effects)*
- *Can therefore use angular “cross-correlations” between reference spectro-z sample and unknown photometric sample to infer redshift distribution of latter*

from J. Helsby

S object with spectroscopic redshift

, photometric object



Cross-Correlation Redshifts

DARK ENERGY
SURVEY

- **See Newman (2008) for the detailed derivation**
- **Here we show the simpler implementation of Menard et al. (2013), Rahman et al. (2015)**
 - **Redshift distribution of unknown photometric sample (“u”) is proportional to angular cross-correlation w_{ur} between it and the reference spectroscopic sample (“r”)**

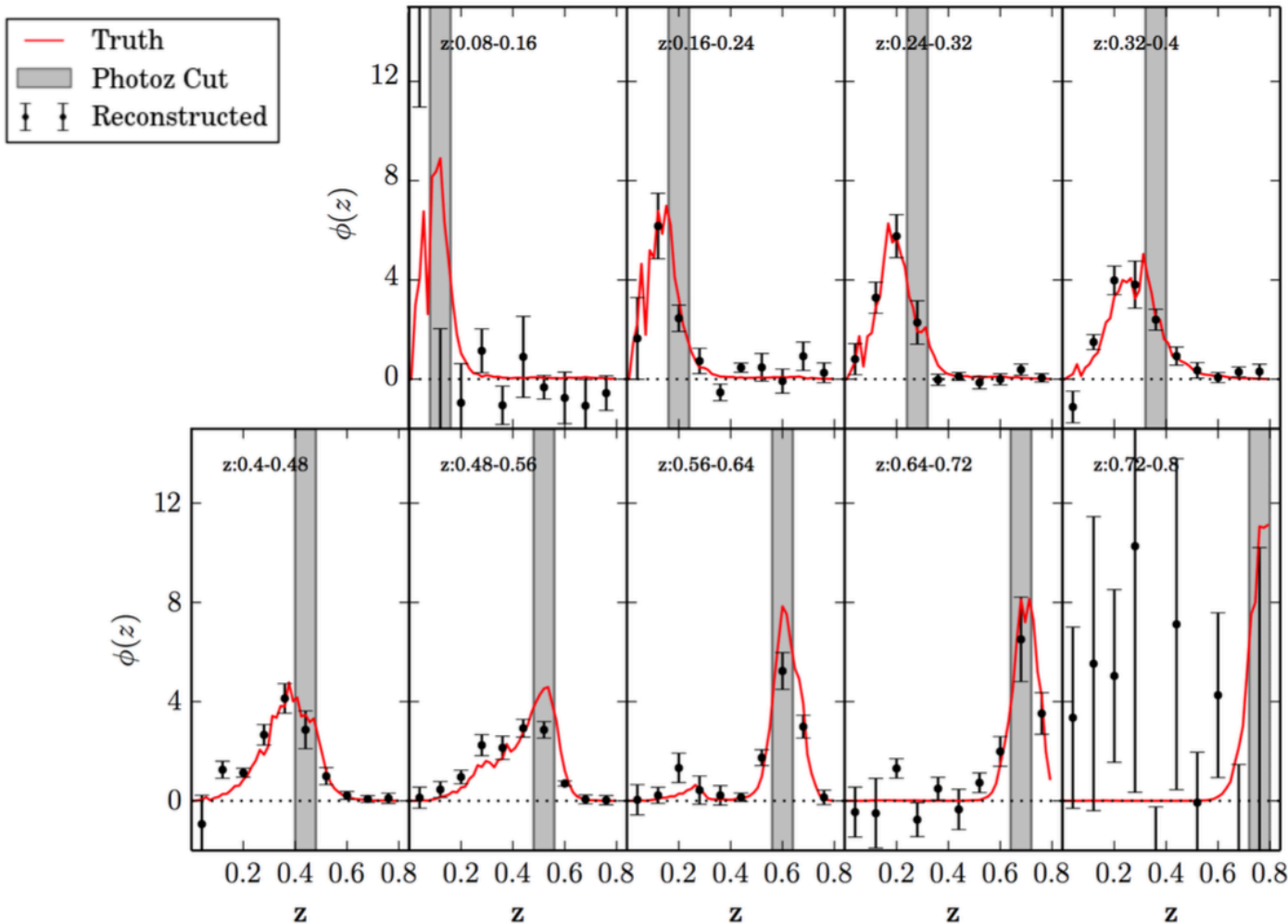
$$dN_u/dz \propto w_{ur}(\theta, z_i)$$

- **The spectro-z sample is split into narrow redshift slices z_i and the angular cross-correlation is computed using the surface density of “u” objects at separation angle θ away from “r” objects with redshift z_i , relative to overall surface density of “u” objects**

$$w_{ur}(\theta, z_i) = \frac{\langle n_u(\theta, z_i) \rangle_r}{n_u} - 1$$

- **Then normalize the redshift distribution by integrating and equating the result to the total number of “u” objects:**

$$\int dz \frac{dN_u}{dz} = N_u$$



Cross-correlation redshift distributions for DES Stripe 82 simulations from J. Helsby thesis (2015)

Figure 4.12: Reconstructed redshift distributions in the mock Stripe 82 for bins of photoz (denoted by gray bars and the photoz cut is written in each panel). Black data points represent reconstructed points via cross-correlation. The true distribution is denoted by the red line. The range of scales considered is $0.003 < \theta < 0.1$ degrees and the reconstruction bin width is $\Delta z = 0.08$. The black dotted line indicates $\phi(z) = 0$.



Cross-Correlation Redshifts

DARK ENERGY
SURVEY

- **Key advantage is that the reference spectro-z samples for cross-correlations do not have to be complete nor be representative of the full photometric sample**
- **But should ideally span the redshift range of the photometric sample**
- **A systematic uncertainty lies in the redshift evolution of bias of photometric sample, if cannot be neglected**
- **Newman et al. (2013) quote calibration requirement on cross-correlation spectro-z sample as “~100,000 objects over several hundred square degrees,” e.g. eBOSS or DESI surveys**
- **Reference sample may even just have (more precise) photo-z’s, like the redMaGiC (Roza et al. 2016) red galaxies we can select from DES over the full footprint, though currently limited to $z < \sim 0.9$**
- **We can supplement with quasar samples that extend to higher redshift**



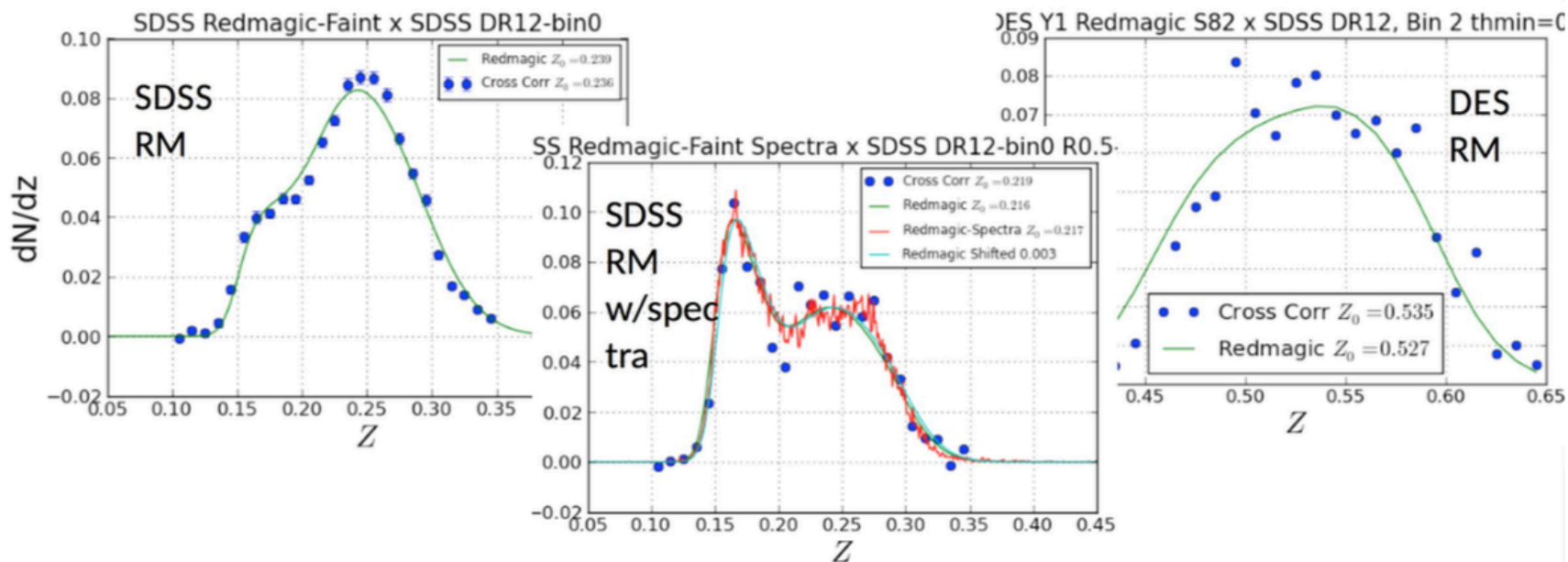
Ross Cawthon

University of Chicago

Cross-correlation redshift results for SDSS and DES redMaGiC samples from R. Cawthon

Calibrating Redmagic w/Cross Correlations

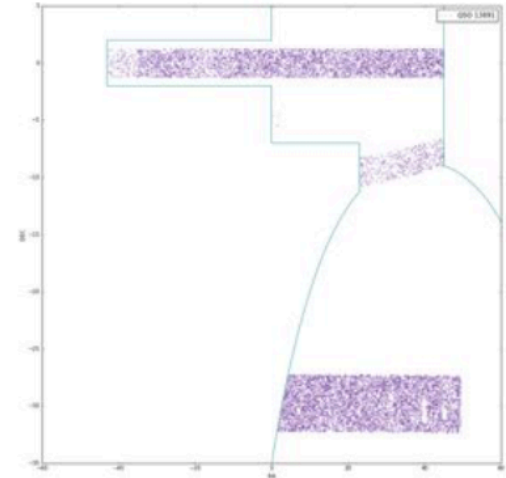
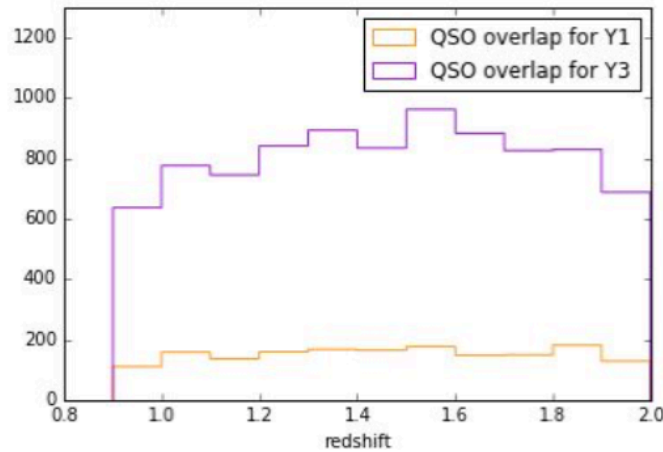
- Some initial work on DES Redmagic x SDSS spectra, have been working more on studying SDSS Redmagic x SDSS spectra
- Fixed some bugs, working on optimizing scales, analyzing different samples in SDSS, starting to get error estimates
- Ongoing work, but results look promising that technique works, low # of spectra w/DES may be limiting



Y3 - potential (already available) spectroscopic samples for clustering-z in the high z regime

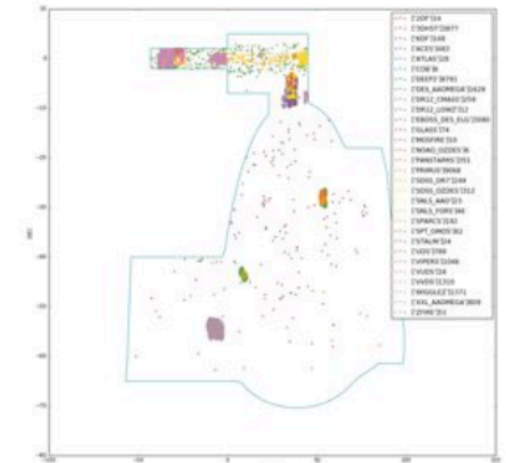
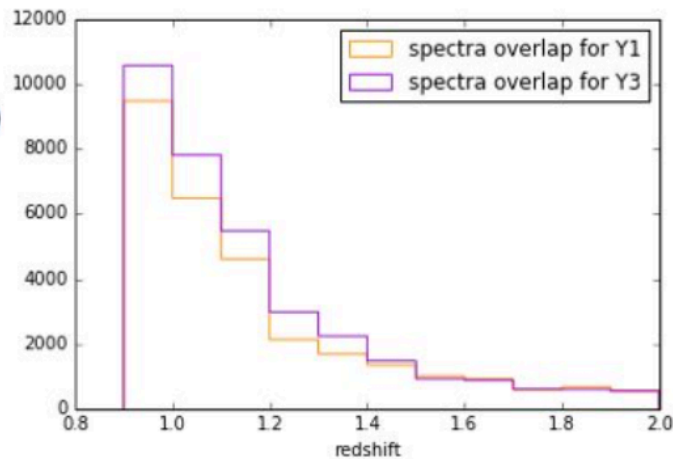
From M. Gatti

QSO: SDSS DR7, 2dFQSO



galaxies (all samples in the plot)

some of the largest samples available: PRIMUS, COSMOS, WIGGLEz, VIPERS, DEEP2, 3DHST





DES Y3 Photo-z Roadmap

DARK ENERGY
SURVEY

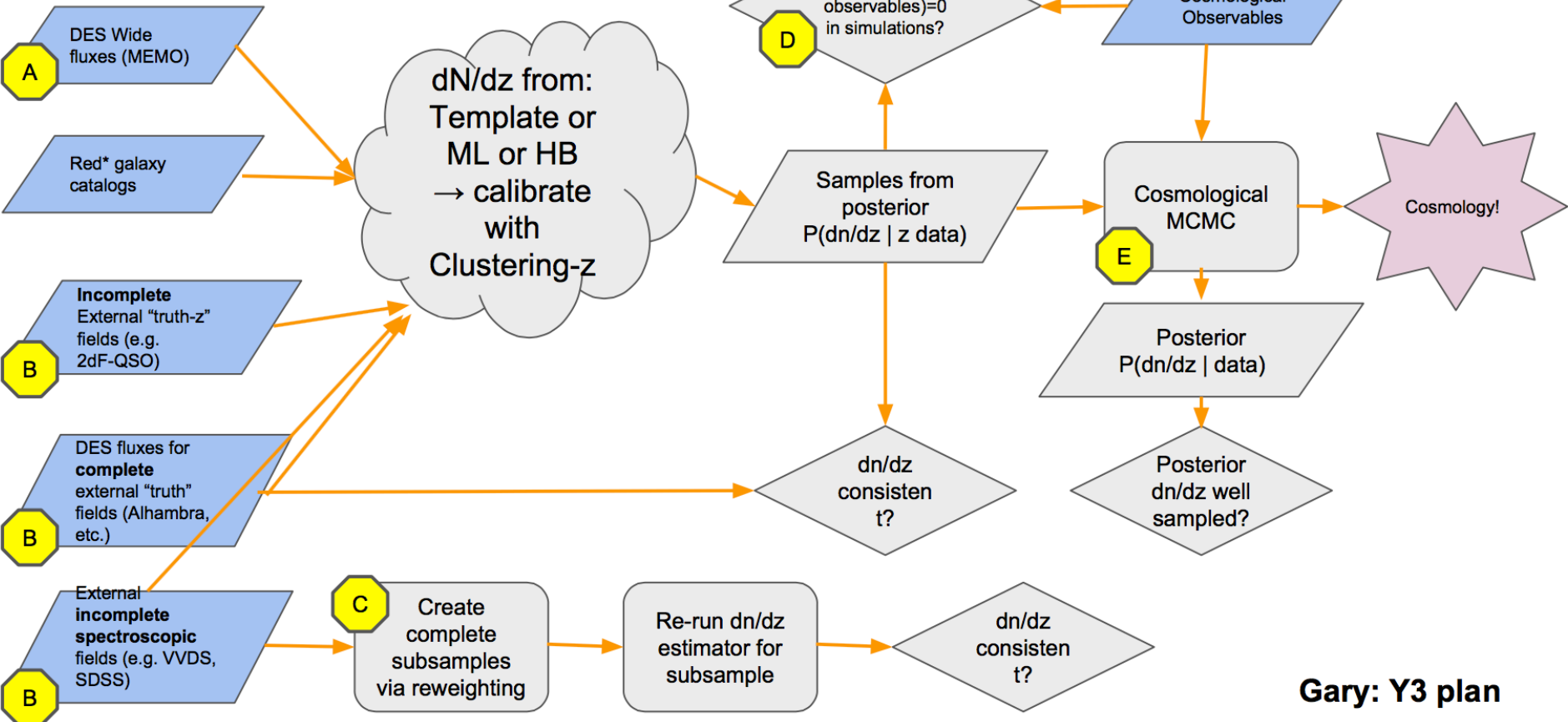
From G. Bernstein and B. Hoyle

Input data

Z estimation

validation

Cosmology
inference



Gary: Y3 plan